博士論文

Solid polymer electrolyte based on polyrotaxane

(ポリロタキサン固体電解質)

林　穎成

Contents

Contents I
List of Figures IV
List of Tables VII
Chapter 1. Introduction 1
Background 1
1.1 Motivation and research scope 2
Chapter 2. Literature review 4
2.1 Polymer electrolyte in the application of lithium ion battery 4
2.1.1 Gel polymer electrolyte (GPE) 4
2.1.2 Solid polymer electrolyte (SPE) 6
2.1.3 Single ion conductor 10
2.2 Polyrotaxane and slide-ring materials 11
2.2.1 polyrotaxane 11
2.2.2 Slide ring material 13
2.2.3 Polyrotaxane and slide ring material in the application of polymer electrolyte 14
Chapter 3. Experimentals 15
3.1 Materials 15
3.2 Characterization Methods 16
Chapter 4. Solid polymer electrolyte based on polyrotaxane 18
4.1 Preparation of SPE 18
4.2 The property of PR based SPE 18
4.3 Functionalization of PR based SPE 24
4.4 Summary 30
Chapter 5. Polyrotaxane based SPE with macromolecular crosslinker 30
5.1 Motivation and research scope 30
5.2 Polyrotaxane based SPE with PEGDE as crosslinker 31
5.2.1 Preparation of PR based SPE with PEGDE 31
5.2.2 The property of PR based SPE with PEGDE 32
5.3 Polyrotaxane based SPE with two-step reaction 35
5.3.1 Two-step synthesis 35
5.3.2 Comparision with cellulose 37
5.4 Summary 40

Chapter 6. Single ion conducting SPE based on polyrotaxane 41
6.1 Motivation and research scope 41
6.2 Synthesis of ionized polyrotaxane 42
6.3 The performance of ionized PR based SPE 44
6.4 Single ion conducting SPE prepared from polyrotaxane graft copolymer 44
6.5 Summary 46
Chapter 7. Summary and future outlook 47
7.1 Summary 47
7.2 Future Outlook 48
References 50

List of Figures

Figure 1. Energy density vs. specific density for various types of rechargeable batteries[3] 1
Figure 2. Plain PEG based SPE easily crystalizes and can be regarded as physically crosslinked material. On the other hand, chemically crosslinked SPE shows good mechanical property and no crystallization but the chain mobility is restricted by the crosslinks. 2
Figure 3. Polyrotaxane that composed of PEG, cyclodextrin and adamantine end-capping group was used to fabricate the slide-ring material with movable crosslinks that provides both good mobility of PEG and mechanical strength of SPE 3
Figure 4. A simple model of lithium ion battery[13] 4
Figure 5. (a) The conduction of lithium ions[18] and (b) the Arrhenius plot of in PEG based SPE[19] 7
Figure 6. The models of physical-crosslinking SPE and chemical-crosslinking SPE[20] 8
Figure 7. the synthesis of segmented networks[21] 9
Figure 8. An example of using PCL and LiBF4 to make the polymer electrolyte[22] 9
Figure 9. (a) polymer electrolyte and (b) polyelectrolyte[24] 10
Figure 10. An example of single ion conductor prepared from triblock copolymer[25] 10
Figure 11. The structure of rotaxane[26] 11
Figure 12. The preparation of polyrotaxane[29] 12
Figure 13. The slide ring material[32] 13
Figure 14. Polyrotaxane in the application of proton exchange membrane of fuel cell[39] 14
Figure 15. GPE prepared from slide ring material[42] 15
Figure 16. The equivalent circuit of SPE in a sandwitch cell with two stainless electrodes 16
Figure 17. (a) The ionic conductivity of polyrotaxane based SPE and (b) the mapping of ionic conductivity as a function of lithium salt concentration and crosslinker feeding. 19
Figure 18. The DSC thermogram of polyrotaxane based SPE 20
Figure 19. (a) Arrhenius plot of PR based SPE fitted by Arrhenius equation and VTF equation and (b) the proposed model of PR based SPE below and upon T_c 21
Figure 20. The proposed model of polyrotaxane based SPE 23
Figure 21. The Arrehnius plot of polyrotaxan based SPE in different crosslinker ratio and the proposed model of polyrotaxane with excess crosslinker 24

Figure 22. The Chemical structure of crosslinker and functionalizing agent used in SPE 24
Figure 23. The stress strain curve and the photos of polyrotaxane based SPE with and without modification of PI..... 25
Figure 24. The proposed model of polyrotaxane based SPE with and without the modification of propyl isocyanate. (a) The CDs are not modified and the SPE is suffered from strong hydrogen bonding. (b) The CDs are excessively modified that leads to an aggregation 26
Figure 25. The SAXS data of polyrotaxane based SPE before and after modification of PI..... 27
Figure 26. The Arrhenius plot of PI modified SPEs..... 28
Figure 27. The DMA result and the Arrhenius plot of PI modified SPEs 29
Figure 28. The proposed model of PR based SPE with macromolecular crosslinker.... 30
Figure 29. The crosslink reaction of PR with EGDE 31
Figure 30. The ionic conductivity of PR with EGDE and PEGDE crosslinker 32
Figure 31. Polyrotaxane based SPE with macromolecular crosslinker in different lithium salt concentration..... 33
Figure 32. (a) The stress-strian curve of SPE with macromolecular crosslinker in different lithium salt concentration (b) the photo of polyrotaxane based SPE crosslinked by PEGDE with 20 wt% LiClO4..... 34
Figure 33. The two-step synthesis of PR bases SPE with macromolecular crosslinker. 35
Figure 34. The ionic conductivity of SPE prepared with pristine polyrotaxane and the two-step synthesis..... 36
Figure 35. The chemical structure of hydroxylpropyl cellulose..... 37
Figure 36. (a) The Arrehnius plot of SPE based on polyrtaxane and cellulose and (b) the proposed model of ion conduction in SPEs..... 38
Figure 37. The DSC thermogram of SPE based on polyrtaxane and cellulose 39
Figure 38. The DMA result of SPE based on polyrtaxane and cellulose 40
Figure 39. (a) The ion transportation in normal lithium battery and (b) the ion transportation in single ion conducter 41
Figure 40. (a)Normal single ion conducting SPE and (b) single ion conducting SPE based on polyrotaxane with ionic group..... 42
Figure 41. The ionization of polyrotaxane 42
Figure 42. NMR result of ionized polyrotaxane..... 43
Figure 43. The ionic conductivity of polyrotaxane based single ion conducting SPE... 44
Figure 44. (a) The model of graft polyrotaxane, “PCLPR” and (b) The synthesis of ionized

PCLPR 45
Figure 45. The ionic conductivity of ionized HAPR and PCLPR based SPE 45
Figure 46. (a)The DSC thermalgram and (b) the proposed model of of ionized graft polyrotaxane based SPR 46
Figure 47. Summary of the research 47
Figure 48. The nanocomposite SPE based on polyrotaxane 49

List of Tables

Table 1. The common used polymer in the application of GPE[15] 5
Table 2. The composition and thermal data of polyrotaxane based SPE..... 22
Table 3. The composition and thermal data of modified polyrotaxane based SPE 24
Table 4. The mechanical properties of PR based SPE with and without modification of PI 25
Table 5. The solubility change after ionization of HAPR 44
Table 6. The solubility change aof PCLPR after functionalization 45

Chapter 1. Introduction

Background

With the growth of emerging technologies, portable devices and electric vehicles (EV) have already played an important role in our daily life. For example, the stock of EV broke the threshold of one million in 2015 where there were only hundreds a decade ago[1]. This trend also promotes the need of battery with light weight, long battery-life and high energy capacity. Lithium ion battery is the most used battery in electronic devices for its high energy dnsity and relatively low cost[2] compared with other conventional rechargeable batteries as shown in **Figure 1**[3]. Commercially available lithium ion batteries are majorly composed of cathode, anode, polymer separator and liquid electrolyte[4]. Even high battery efficiency can be achieved with this design, the short-circuit caused by the formation of lithium dendrite shows a great concern for battery safety. The growth of lithium dendrite in liquid electrolyte might break the polymer separator, make a direct contact between anode and cathode, and cause an explosion[5].

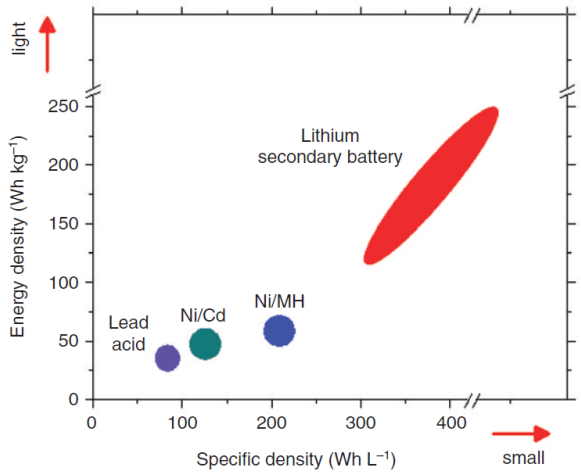

Figure 1. Energy density vs. specific density for various types of rechargeable batteries[3]

Solid polymer electrolyte (SPE) was first discovered in 1970s[6] by Fenton and his coworkers who dissolved the alkali salts into Poly(ethylene glycol) (PEG). It is a relatively new research topic in polymer materials which allows many important and new applications to be achieved such as lithium battery, fuel cell, and dye sensitized solar

cell[7]. The use of solvent-free SPE as separator as well as electrolyte in lithium battery was proved to suppress the growth of lithium dendrite[8]. Furthermore, batteries can also be made lighter and flexible with SPE[9]. However, the ionic conductivity of SPE is too low to be commercialized yet[10].

1.1 Motivation and research scope

The two main factors required for achieving high ionic conductivity of SPE are high mobility of polymer chains and high dissociating efficiency of lithium salt[11]. PEG is the most studied SPE material because it perfectly fits these two criteria. The backbone ether bonds in PEG provides flexibility and hence high chain mobility[12] and dipole moment leading to high dissociating efficiency of lithium salt. However, the most of PEG crystalizes and loses mobility, and thus lowers the conducting efficiency of lithium ions. This is the reason why the ionic conductivity of PEG based SPE is normally low at ambient temperature but shows a drastic enhancement above the melting temperature of PEG. Preventing the crystallization of PEG seems to be inevitable to enhance the ionic conductivity, but the crystalline structure also provides the good mechanical strength as shown in **Figure 2** (a). This contradiction can be solved in some degree by chemically crosslinking PEG, which enhances the mechanical strength and also restricts the crystallization of PEG as shown in **Figure 2** (b). However, still crosslinking slows down the motion of polymer chains and makes the ionic conduction inefficient. A new method which can maintain the chain mobility of polymer without losing mechanical strength is desired in the future development of SPE.

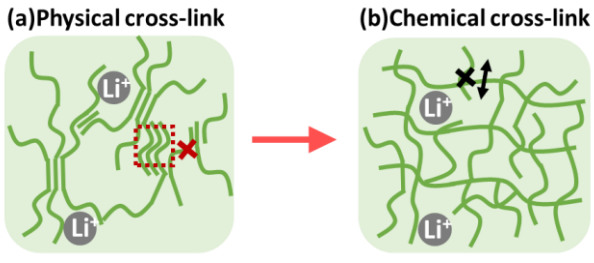

Figure 2. Plain PEG based SPE easily crystalizes and can be regarded as physically crosslinked material. On the other hand, chemically crosslinked SPE shows good mechanical property and no crystallization but the chain mobility is restricted by the crosslinks.

To solve the contradiction between the mobility of polymer chain and mechanical strength of SPE, we proposed the idea of using “polyrotaxane” to prepare SPE in this work. Polyrotaxane is a supramolecular polymer that comprises a linear polymer chain threading through several cyclic molecules. The cyclic molecules are not chemically bonded to the linear polymer chain but topologically constrained by the linear polymer and interlocked by the bulky end-capping group as shown in **Figure 3** (a). Since the cyclic molecules are not chemically connected to the axis polymer, a unique “mobile crosslink” that allows the sliding of axis polymer chain can be obtained by connecting these cyclic molecules. In this thesis, polyrotaxane comprised of PEG and alpha-cyclodextrin (α-CD) was selected to make the SPE, in which PEG can contributes to the ionic conduction and the interlocked cyclodextrins can form the mobile crosslinks as shown in **Figure 3** (b). The mobility of PEG is expected to be maintained because α-CDs can prevent the PEG backbone from crystallization and the crosslinks does not anchor the axis PEG.

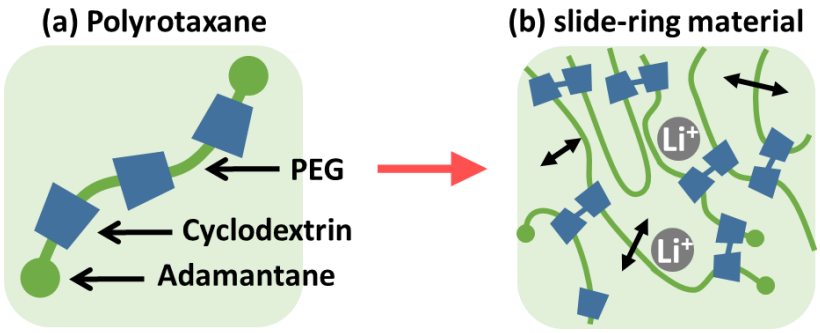

Figure 3. Polyrotaxane that composed of PEG, cyclodextrin and adamantine end-capping group was used to fabricate the slide-ring material with movable crosslinks that provides both good mobility of PEG and mechanical strength of SPE

Chapter 2. Literature review

2.1 Polymer electrolyte in the application of lithium ion battery

2.1.1 Gel polymer electrolyte (GPE)

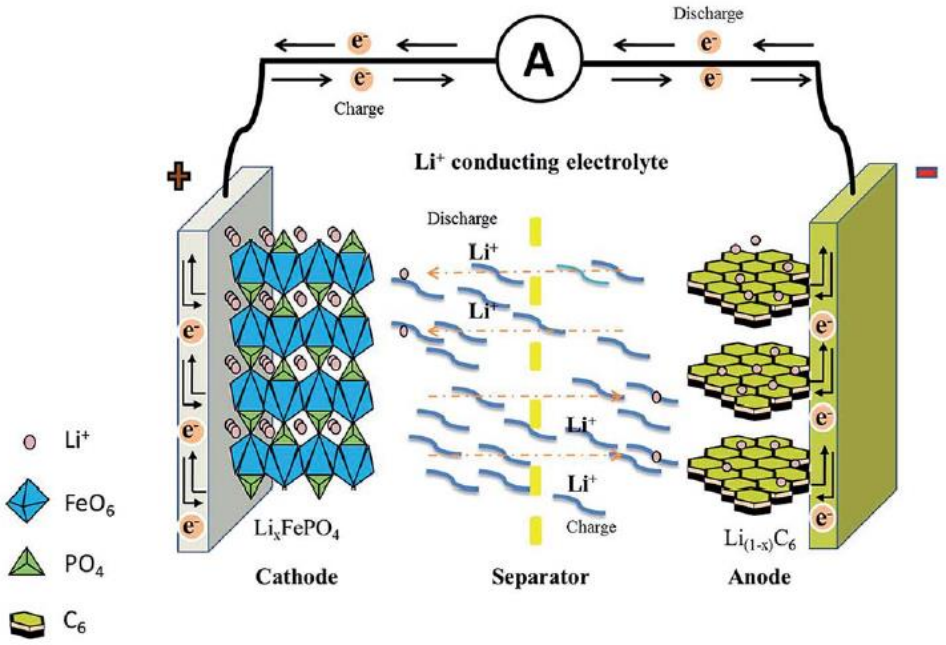

Figure 4. A simple model of lithium ion battery[13]

Figure 4 shows a simple model of lithium ion battery. The lithium ion battery is mainly composed of cathode, anode, and the polymer electrolyte. In the commercially available lithium ion battery, the polymer electrolyte is actually indicating the polymer separator that is swelled by the liquid electrolyte and is also known as the gel polymer electrolyte (GPE). The polymer separator should be *a microporous layer consisting of either a polymeric membrane or a non-woven fabric mat*[14] that allows the uptake of liquid electrolyte and the transportation of lithium ions. So, even the GPE can provide a high ionic conductivity for SPE, the safety issue resulted from the low mechanical strength is always needed to be concerned.

Polymer separator

Table 1. The common used polymer in the application of GPE[15]

Polymer matrix	Molecular structure	Tg* (°C)	Tm** (°C)	Problems facing
PAN	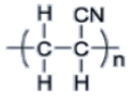	125	317	Severe passivation upon contact with lithium metal anodes
PMMA	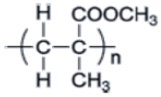	105	amorphous	Low mechanical strength
PVC	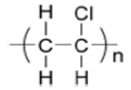	80	220	Low ionic conductivity and compatibility towards lithium metal anodes
PVDF	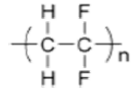	-40	171	Poor interfacial properties with lithium metal anodes and the formation of LiF

*T_g = glastransition temperature
**T_m = melting point

The polymer separator used in GPE should provide sufficient mechanical strength, good uptake of solvent, thermal and chemical stabililty and good compatibility to the electrode. The porosity is also needed to be considered. If there are more pores in the polymer matrix, more liquid electrolytes can be included and the ionic conductivity can be enhanced. However, the mechanical strength of polymer separator will also be lowered with high porosity. **Table 1** shows the polymers that are commoly used in the fabrication of GPE, including PAN, PMMA, PVC and PVDF. It is noteworthy that most of the SPE based on single polymer matrix can not meet the requirement to lithium ion battery. Poymer blends or copolymers are usually used to improve the property of polymer matrix of GPE.

Liquid electrolyte

The liquid electrolyte is usually prepared from lithium salt and organic solvent. For example, the liquid electrolyte made from lithium hexafluorophosphate ($LiPF_6$) and the

mixed solution of ethylene carbonate (EC) and propylene carbonate (PC) that shows high dielectricity and ionic conductivity is extensively studied[10]. Recently, due to the safety concern and the market demand of lithium battery with high energy density, ionic liquid with good chemical and thermal stability becomes popuplar in the choose of liquid electrolyte.[16]

2.1.2 Solid polymer electrolyte (SPE)

In gel polymer electrolyte, the role of the polymer separator is to prevent the direct contact between the electrodes and to keep the liquid electrolyte from leaking. The polymer separator is not involved in the conduction of lithium ions. So, the thinner the polymer separator is, the higher the ionic conductivity can be. However, the mechanical strength of the ultra-thin polymer separator becomes even lower when soaked in the liquid electrolyte and causes a great safety concern. For example, a smart phone of Samsung was recalled and banned from the airline flights recently due to the exploding of the battery which was resulted from the fracture of polymer separator[17]. On the other hand, solid polymer electrolyte which is a solvent free polymer membrane can not only separate the electrodes but also conduct the lithium ions. Safer, flexible and lighter battery can be achieved with SPE.

PEG based SPE

(a)

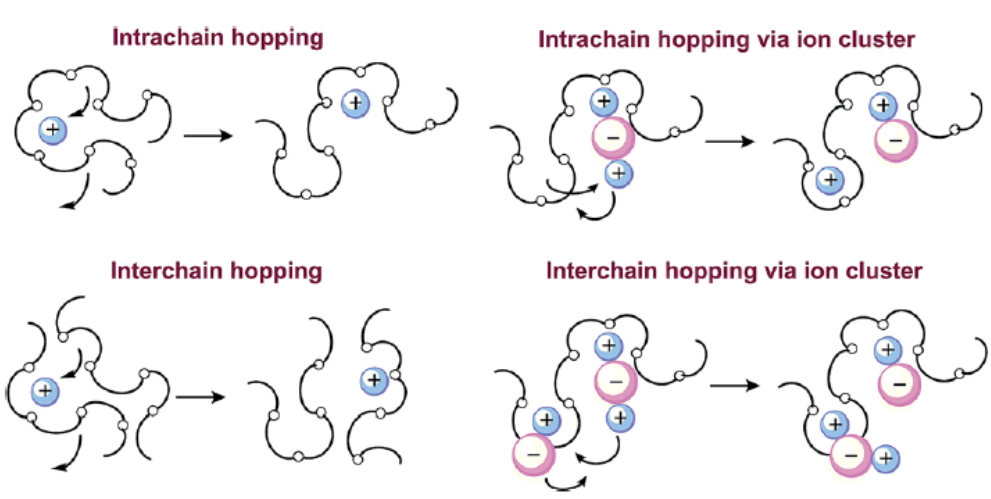

(b)

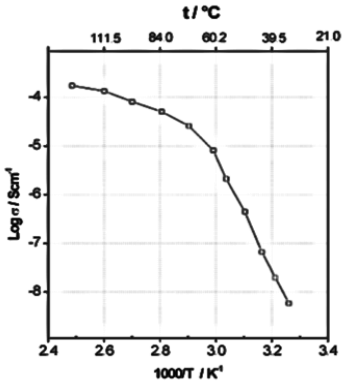

Figure 5. (a) The conduction of lithium ions[18] **and (b) the Arrhenius plot of in PEG based SPE**[19]

PEG is the most studied polymer material of SPE because of its high flexibility, dielectricity and the ability to solvate the lithium ions. The ethylene oxide (EO) unit also shows a high donor number for lithium ions[18]. Figure 5 (a) shows the fast lithim ion transportation in PEG matrix. However, PEG is very easy to crystallize due to the uncomplex structure. The crystalline of PEG will restrict the fast lithim ion transportation, so the ionic conductivity of PEG based SPE usually shows a low ionic conductivity at room temperature as shown in Figure 5 (b).

The improvement of PEG based SPE

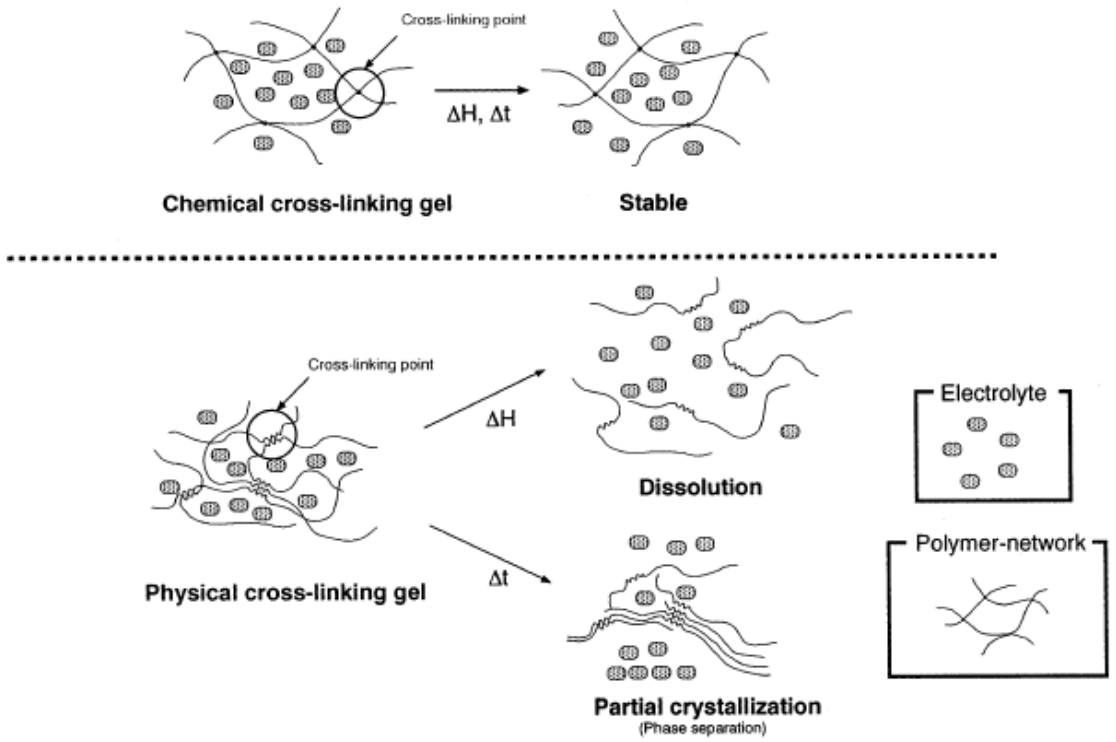

Figure 6. The models of physical-crosslinking SPE and chemical-crosslinking SPE[20]

Crosslinking is a common way to enhance both the mechanical property and the ionic conductivity by preventing the crystallization of PEG based SPE. The chemical crosslinked SPE is *thermally stable over time, where the physical crosslinking SPE tends to swell and dissolve with heat (ΔH), and leaks solution from the structure with time (Δt)* as shown in **Figure 6**[20]. The crosslinks in SPE have ensured the long-term stability and cycle life of battery. There is also another approach of making PEG based SPE with a segmented block copolymer network as shown in **Figure 7**. By incorporating with a different kind of polymer, the degree of crystallinity and T_g of PEG can be reduced. And the crosslink can also stabilize the phase between the different polymers. The SPE prepared from PMMA and PEG segmented block copolymer network shows a high ionic conductivity at room temperature of 6×10^{-5} S/cm

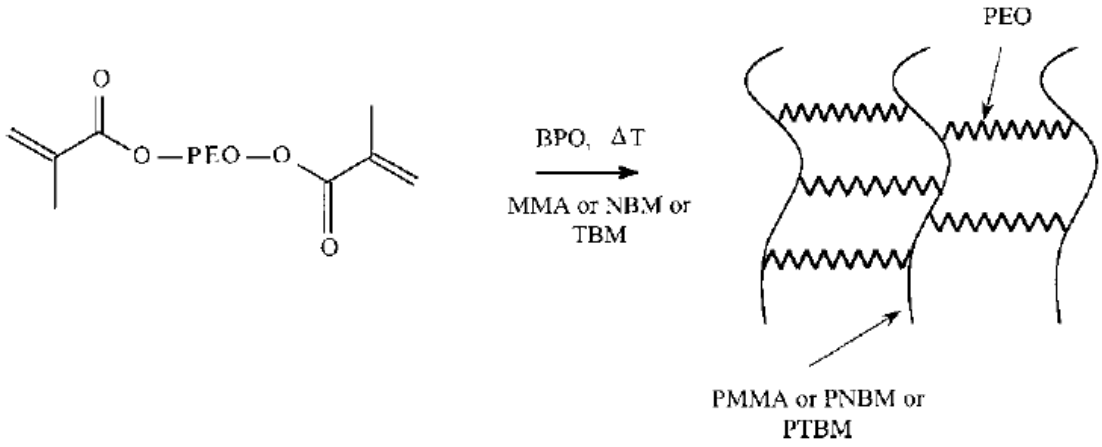

Figure 7. the synthesis of segmented networks[21]

Other SPEs

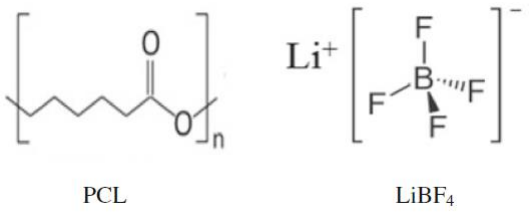

Figure 8. An example of using PCL and LiBF4 to make the polymer electrolyte[22]

Besides PEG, there are lots of polymer materials that have been used as SPE materials[23]. For example, biodegradable non-toxic PCL is one of the commonly used SPE material because it shows low glass transition temperature and the carboxide group of PCL can coordinate with lithium ions[22].

2.1.3 Single ion conductor

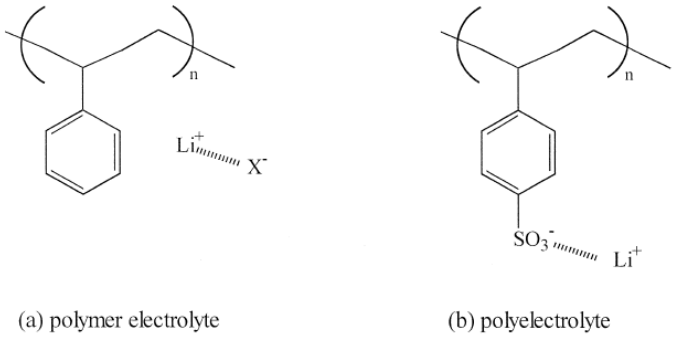

Figure 9. (a) polymer electrolyte and (b) polyelectrolyte[24]

Except for the normal polymer electrolyte as shown in **Figure 9 (a)**, there is another special type of solid polymer electrolyte that is called the single ion conductor which is prepared from the polyelectrolyte as shown in **Figure 9 (b)**. The single ion conducting polymer electrolyte shows some advantage in the fabrication of lithium battery. By fixing the anions covalently to the polymer, the transference number can be enhanced since the concentration gradient resulted from the difference in diffusivity of lithium ion and its counter ion is eliminated. But the the ionic crosslink between the attached functional group restrict the mobility of the polymer chain and causes low ionic conductivity of SPE. Block copolymer with an ionized block as the source of lithium ion and a flexible ion conducting block is often used to enhance the ionic conductivity of SPE as shown in **Figure 10**[25].

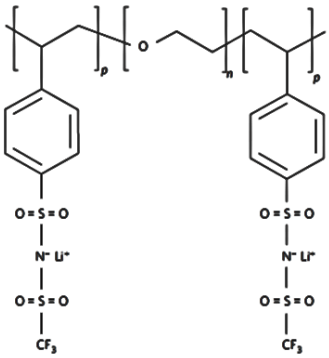

Figure 10. An example of single ion conductor prepared from triblock copolymer[25]

2.2 Polyrotaxane and slide-ring materials

2.2.1 polyrotaxane

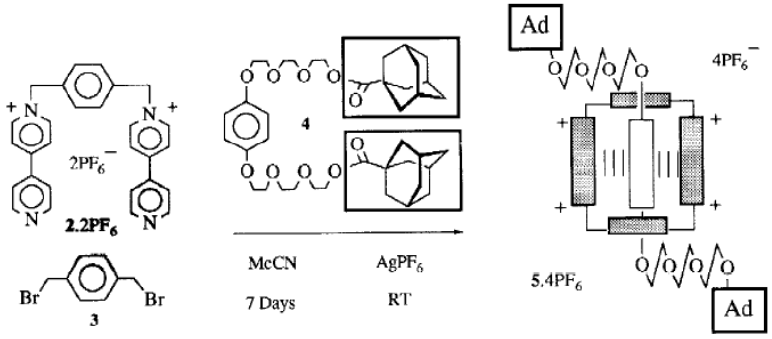

Figure 11. The structure of rotaxane[26]

The 2016 nobel prize was awarded to the molecular machine[27]. However, it is not a very new idea. The concept of building “machines” with atoms has been proposed early in 1959. But it was not until the progress in supramolecular chemistry, the molecular machine has become possible. In 1983, Jean-Pierre Sauvage and his co-workers synthesized the superamolecular catenanes and rotaxanes in a good yield with metal coordination[28] and opened up the field of topological chemistry. One of the most representative superamolecule is rotaxane which is composed of cyclic molecules threaded by a molecular chain with bulky end groups. Figure 11 is an example of the molecular machine made from the rotaxane that the interlocked cyclic molecules can move along the axis chain molecule.

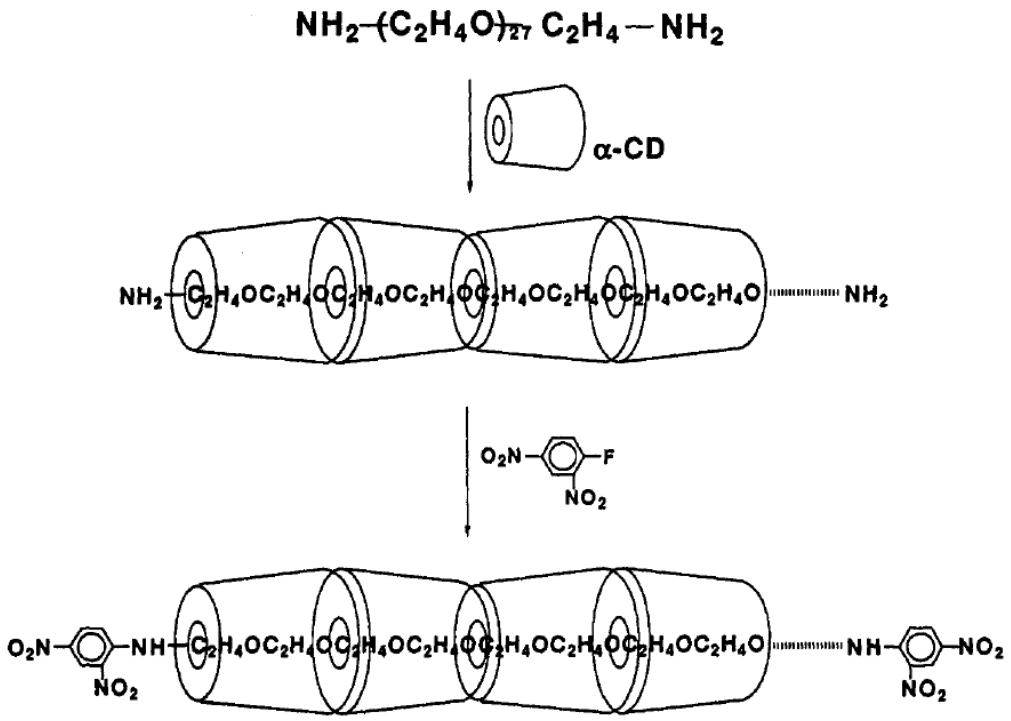

Figure 12. The preparation of polyrotaxane[29]

Besides the rotaxane made from metal coordination, there is another type of rotaxane that is prepared from α-cyclodextrins and poly(ethylene glycol) (PEG) which is discovered by Harada et al.[29] and named as the polyrotaxane. **Figure 12** shows how the polyrotaxane was prepared by adding PEG into the saturated aqueous solution of α-cyclodextrins followed by end-capping. This kind of polyrotaxane has a great potential in the application of biomedical material such as scaffold material, bio-sensor, drug delivery[30] and gene delivery[31].

2.2.2 Slide ring material

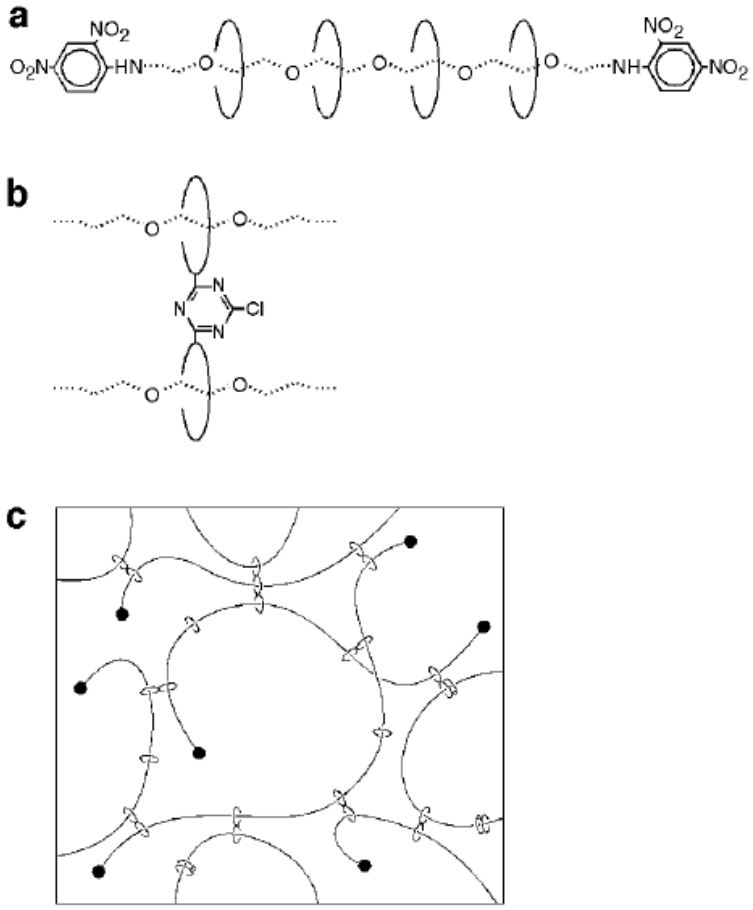

Figure 13. The slide ring material[32]

The sucess of synthesizing polyrotaxane with PEG and α-cyclodextrins in a high yield has attracted many people's attention. Lots of polyrotaxane related research was then being studied[33]. Ito et al.[32] used cyanuric chloride to crosslink the polyrotaxane to make a polyrotaxane gel featureing with figure-of-eight crosslink which is also known as the "slide-ring gel" as shown in **Figure 13**. The mobile crosslink can move freely like pulleys which has never been found in conventional physical or chemical crosslinking material. And the unique propery of slide-ring material such as self-healing[34][35] or high damping property[36] shows good potential in the application of all kinds of area including biomedical[37], and electronic materials[38].

2.2.3 Polyrotaxane and slide ring material in the application of polymer electrolyte

Polyrotaxane has already been used in some applications of polymer electrolyte for lithium battery or other purpose. Here we will show some examples. Figure 14 shows the the proton exchange membrane prepared from PVA with the addition of polyrotaxane in the application of fuel cell. The polyrotaxane plays a role like the ionic channel but also prevents the crossover of methanol. The proton conductivity increased with the addition of polyrotaxane. The addition of polyrotaxane shows a good potential in the fabrication of proton exchange membrane for direct methanol fuel cell.

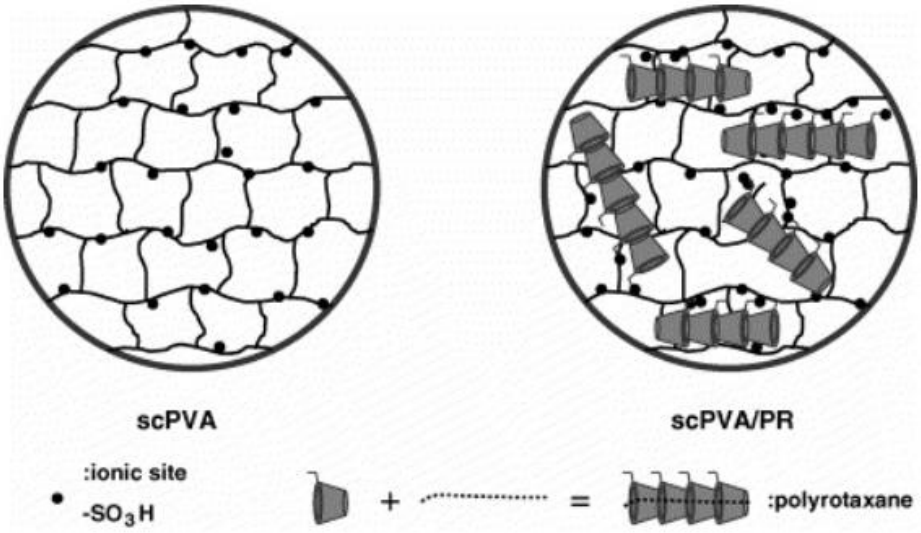

Figure 14. Polyrotaxane in the application of proton exchange membrane of fuel cell[39]

In Figure 15, an example of gel polymer electrolyte prepared from the slide-ring material swollen by the lithium ion based ionic liquid was shown. The use of slide-ring material has provided a good absorption of ionic liquid which leads to the high ionic conductivity[40]. The slide ring gel also shows a good puncture resistance as high as 1000% in puncture elongation[41]. The puncture resistance is an important factor that promises the safety of lithium battery. But according to the best of our knowledge that there is no research on the SPE based on slide ring materials.

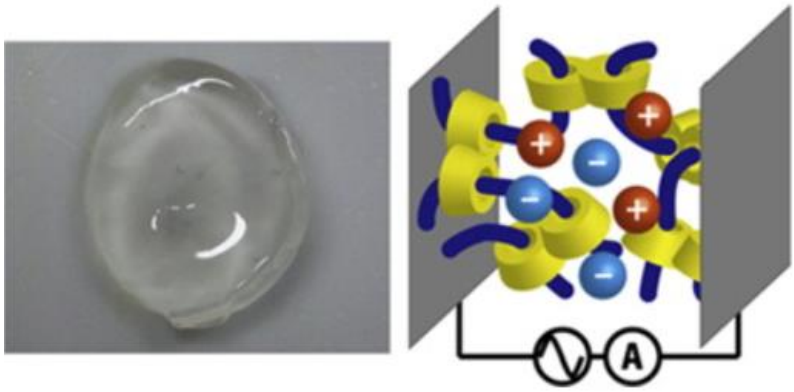

Figure 15. GPE prepared from slide ring material[42]

Chapter 3. Experimentals

3.1 Materials

Polyrotaxane (HAPR35, purity>99%) with the axis PEG in the molecular weight of 35,000 and approximately 100 α-CD threaded by the PEG was purchased from Advanced Softmaterials Inc (Tokyo, Japan). In Chapter 4, we dissolve the polyrotaxane and battery grade lithium perchlorate ($LiClO_4$, purchased from Sigma Aldrich) to super dehydrated *N*,*N*-dimethylformide (DMF, purchased from TKS.) followed by adding hexamethylene diisocyanate (HMDI, purchased from TKS) or a mixture of HMDI and propyl isocyanate (PI, purchased from Sigma Aldrich) to obtain the solution for solvent casting.

In Chapter 5, ethylene glycol diglycidyl ether (EGDE, purchased from TKS) or poly(thylene glycol) diglycidyl ether (PEGDE, purchased from Sigma Aldrich) (MW=500) was used as the short and macromorecular crosslinker, respectively. Carbonyldiimidazole (CDI, purchased from TKS) was blended with poly(thylene glycol) (PEG, purchased from Sigma Aldrich) (MW=1000) to form the macromolecular crosslinker for two-step synthesis. Hydroxypropyl cellulose (H-cellulose, purchased from Sigma Aldrich) was used as a reference material foe two-step synthesis.

Lithium Hydroxide (LIOH, purchased from Sigma Aldrich) and 1,3-Propane sultone (purchased from Sigma Aldrich) were used to functionalize the polyrotaxane in Chapter 6. Graft polyrotaxane with poly(ε-caprolactone) (PCLPR, purity>99%) with the axis PEG of a molecular weight of 35,000 and approximately 100 α-CD threaded by the PEG was purchased from Advanced Softmaterials Inc (Tokyo, Japan).

3.2 Characterization Methods

Electrochemical impedance spectra (EIS)

The ionic conductivity measurement[43] was carried out using a Biologic SP-150 electrochemical workstation. The SPE membrane was settled in a T-shape cell and sandwiched by two stainless steel electrodes that connects to the electrochemical workstation. Nyquist plot of electrochemical impedance spectra (EIS) was measured from 100 mHz to 1 MHz at the sinusoidal voltage amplitude of 500 mV. In the Nyquist plot, a semicircle can be observed at high frequency that is from the *parallel combination of a resistor(R_b) and constant phase element (CPE)*[44]. And the tilted spike observed at low frequency could also be represented by another CPE connected in series[45]. We can obtain the resistance by fitting the Nyquist plot with an equivalent circuit[46].

The ionic conductivity (σ) can thus be obtained by

$$\sigma = \frac{L}{R_b \times A} \tag{3.1}$$

where L is the thickness of the SPE membrane, R_b is the ohmic resistance of SPE and A is the interface area between the electrode and the SPE membrane.

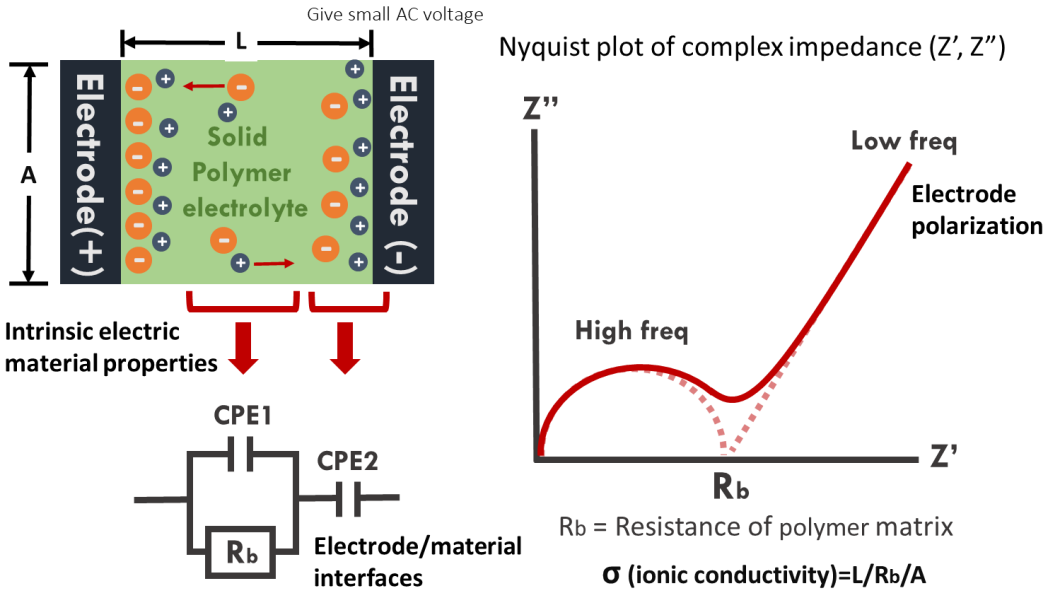

Figure 16. The equivalent circuit of SPE in a sandwitch cell with two stainless electrodes

Nuclear magnetic resonance (NMR)

1H spectra were obtained from JNM-AL400(JEOL) spectrometer at 400 MHz with deuterated Dimethyl sulfoxide (DMSO-*d6*, 99.8 %) from Aldrich as solvent.

Differential scanning calorimeter (DSC)

The degree of crystallinity (X_c) was calculated from the enthalpy (ΔH_m) of melting measured by differential scanning calorimeter (DSC) with the equation,

$$X_c = \frac{\Delta H_m}{\Delta H_m{}^0{}_{(PEG)}} \tag{3.2}$$

in which $\Delta H_m{}^0{}_{(PEG)}$ is the heat of fusion of 100% crystalline PEG (202.4 J/g)[47]. The DSC measurement was performed with a Hitachi DSC 7000X from -50°C to 150°C at the heating rate of 10°C /min.

Dynamic mechanical analysis (DMA)

Dynamic mechanical analysis (DMA)was carried out by TA Instrument RSA-III. Storage (E') and loss (E") moduli were measured using a 10 mm*2 mm rectangular shape specimen at the angular velocity of 6.2832 rad/s from 25 to 125 ℃.

Tensile test

The stress strain curve was measured by Shimadzu EZ-S under a strain rate of 33% /min.

Small-angle X-ray scattering (SAXS)

Small-angle X-ray scattering (SAXS) experiments were performed at Photon Factory (KEK, Tsukuba, Japan).

Chapter 4. Solid polymer electrolyte based on polyrotaxane

4.1 Preparation of SPE

HAPR and battery grade lithium perchlorate ($LiClO_4$) were first dissolved in super dehydrated *N*,*N*-dimethylformide (DMF) Then hexamethylene diisocyanate (HMDI) and Propyl isocyanate (PI) were added to the solution under vigorously stirring for 12 hours. The mixed solution was poured into a Teflon petri dish and dried at 80 °C for 12 hours to obtain the SPE membrane. The membrane was then evacuated at 80 °C for 24 hours to remove the residual solvent and then heated at the highest measuring temperature (150 °C) for 30 minutes to ensure no side reaction will occur during the electrochemical measurements. The thickness of the membrane is approximately 150 μm. All the chemicals were used as received.

4.2 The property of PR based SPE

(a)

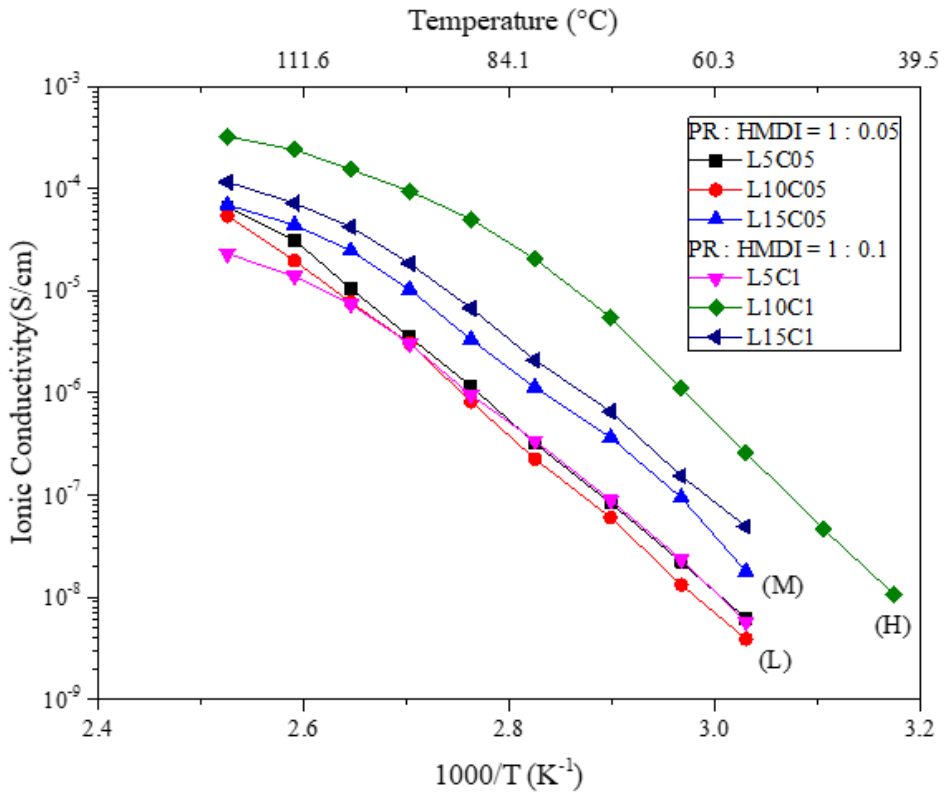

(b)

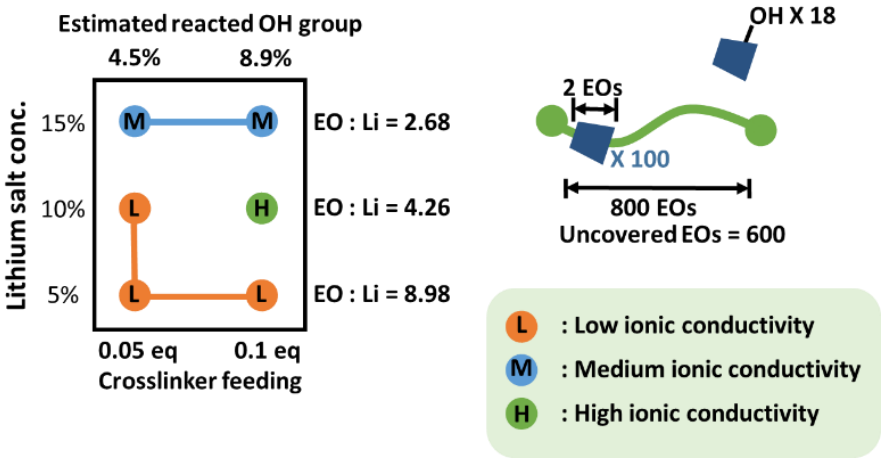

Figure 17. (a) The ionic conductivity of polyrotaxane based SPE and (b) the mapping of ionic conductivity as a function of lithium salt concentration and crosslinker feeding.

Figure 17 (a) shows the ionic conductivities of polyrotaxane based SPEs. The labels of the samples represent the lithium salt concentration and the crosslinker-feeding ratio to polyrotaxane. For example, the sample with 5 wt% of LiClO4, 1 gram of polyrotaxane and 0.1 gram of HMDI was named as L5C1. The compositions of other samples are listed in Table 1. The polyrotaxane based SPEs are classified into three groups of low (L), medium (M) and high (H) ionic conductivities as shown in **Figure 17** (b). In group L, the SPE shows the lowest ionic conductivity and almost constant slope in the Arrhenius plot which is different from the common PEG based SPE. Group L includes the SPE with either low crosslinker-feeding or low lithium salt concentration. In group M, the ionic conductivity of SPE is slightly higher than those in group L and the slope of ionic conductivity as a function of inverse temperature changes at around 100°C. It is majorly composed of the sample with high lithium salt concentration. In group H, it contains only the SPEs with moderate lithium salt and high crosslinker-feeding ratio which shows the highest ionic conductivity among all the other SPEs. The change of slope in Arrhenius plot was at 70°C which was much lower than the other samples but still higher than PEG based SPE. To clarify the difference, thermal properties were measured by DSC.

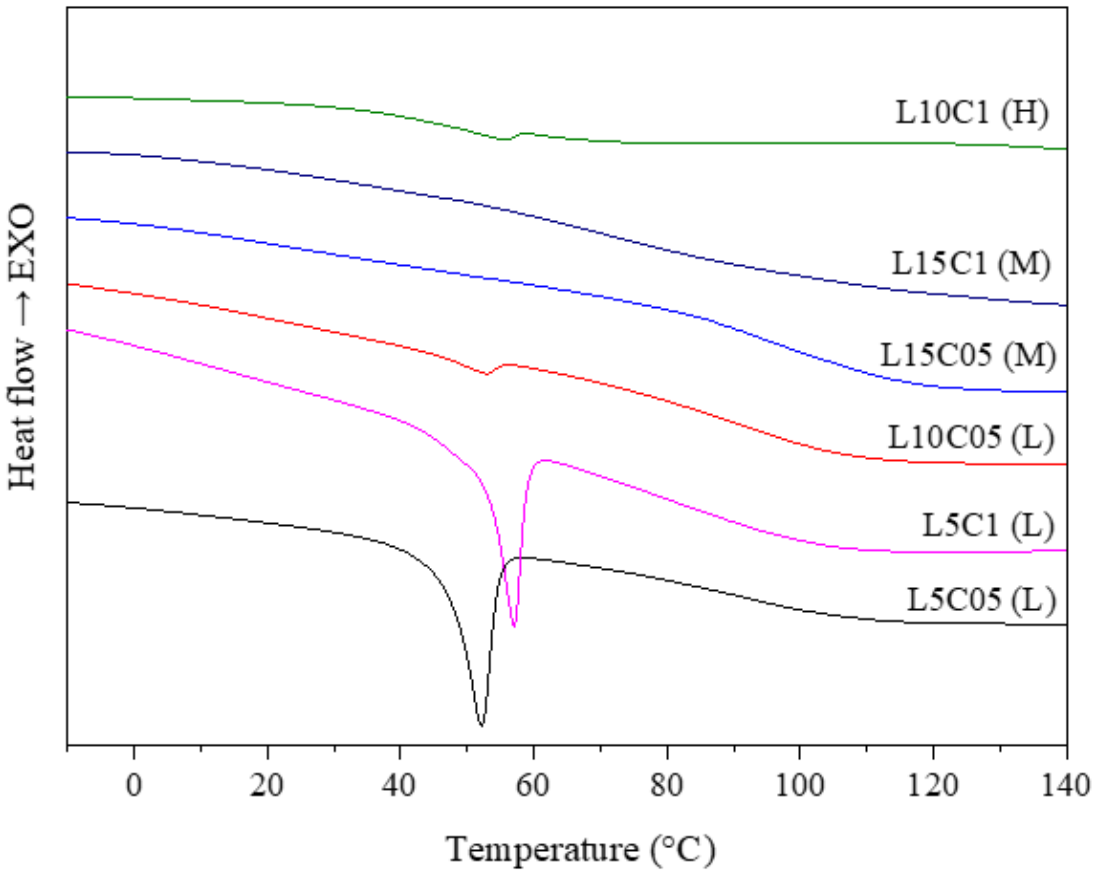

Figure 18. The DSC thermogram of polyrotaxane based SPE

Endotherms due to melting of PEG are found in some of the crosslinked PRs in **Figure 18**. However, the crystallinity of polyrotaxane is only 3.1%, which is negligible fraction compared to pure PEG (100%) and crosslinked PRs have even lower crystallinity as shown in **Table 2**. Therefore, crystallization of PEG is prevented effectively by inclusion with CDs and crystallinity is no longer the determining factor of ionic conductivity. For example, L10C05 and L10C1 show a large difference in ionic conductivity but they share similar crystallinity. We can conclude that the crystallization of PEG has been significantly reduced by inclusion complex formation and was almost negligible in all the samples. In **Figure 18**, instead of a crystalline peak, a very broad glass transition ending at 100°C can be observed in DSC thermogram. The glass transition of PEG is in general very low, i.e. -100°C, and is not usually observed due to high crystallinity. The origin of the glass transition in polyrotaxanes is still an open question and actively studied[48]. The most probable origin of the glass transition is the frozen movement of CDs[49]. The rigid framework of frozen CDs also restricts the movement

of PEG. In particular, the hydrogen bonding between CDs increases the intermolecular interaction between CDs and causes higher glass transition temperature.

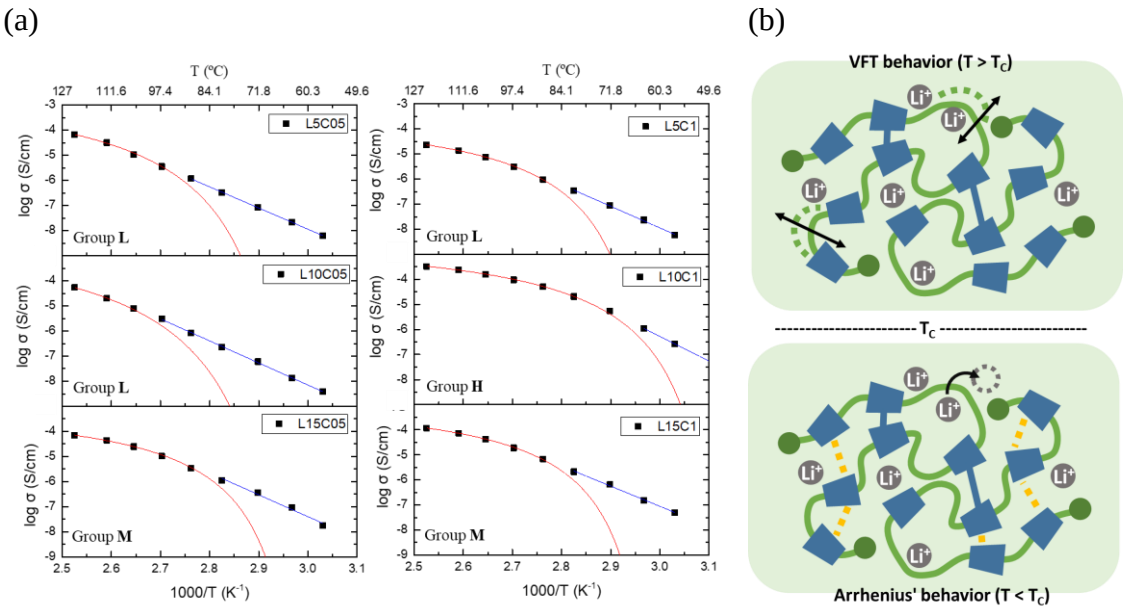

Figure 19. (a) Arrhenius plot of PR based SPE fitted by Arrhenius equation and VTF equation and (b) the proposed model of PR based SPE below and upon T_c

The relationship between temperature and ionic conductivity is often described with the empirical equations. In the PR based SPE, the ionic conductivity can be fitted by a combination of Arrhenius equation and Vogel-Tammann-Fulcher (VTF) equation[50] as shown in Figure 19 (a). In the low temperature area of the plot, the ionic conductivity shows a linear feature that can be perfectly fitted by the Arrhenius equation. It suggests that the conduction was from the hopping of ions to the neighboring vacancies[51] but not related to the motion of the polymer chain. In the high temperature area, the ionic conductivity is no longer linear but the curve follows the VTF behavior[52]

$$\sigma = AT^{\frac{-1}{2}} exp\left[\frac{-B}{k_B(T-T_0)}\right] \quad (4.1)$$

where A is a constant related to the charge density, B is the activation energy related to the mobility of polymer chain, k_B is the Boltzmann's constant, and T_0 is the equilibrium

glass transition[53] temperature which is usually 50°C lower than the real glass transition temperature. The VTF equation was originally used to describe the viscosity of glasses[53], but was also applied to describe the relationship between temperature and ionic conductivity in polymer electrolyte. We also set the critical temperature that the ionic conductivity changes from the Arrhenius behavior to VTF behavior as T_c[54]. As we have mentioned, the hydrogen bonded CDs reduce the mobility of PEG and causes higher glass transition temperature and may also directly trap lithium ions and hence reduce the conductivity. So, the conductivity is very low and follows the Arrhenius behavior in PR based SPE. When the temperature of the SPE is higher than T_c, the hydrogen bond between CDs is weakened and the PEG chain performs segmental motion. The conductivity is enhanced and shows the VTF behavior because the lithium ions are able to move along with the PEG chain as shown in Figure 19 (b).

Table 2. The composition and thermal data of polyrotaxane based SPE

		composition		Ionic conductivity				DSC		
sample	group	wt% $_{LiClO4}$ (%)	PR:HMDI	T_C (°C)	A ($SK^{0.5}$/cm)	B (eV)	T_0 (°C)	T_m (°C)	Xc $_{PEG}$ (%)	Xc $_{PR}$ (%)
PEG		0	--		--	--	--	65.4	100	--
PR		0	--		--	--	--	56.9	3.1	100
L5C05	L	5	10:0.5	97	0.129	0.026	57.2	52.4	2.2	70.3
L10C05	L	10	10:0.5	105	0.252	0.031	57.1	53	0.16	5.1
L15C05	M	15	10:0.5	89	0.024	0.016	56.8	--	--	--
L5C1	L	5	10:1	89	0.011	0.018	56.3	58.9	1.4	46.6
L10C1	H	10	10:1	72	0.092	0.018	42.1	55.9	0.18	5.9
L15C1	M	15	10:1	89	0.038	0.016	57.0	--	--	--

When the amount of crosslinker concentration increased and hence more hydroxyl groups on the CDs were substituted such as L10C1, the intermolecular interaction between CDs was reduced and a lower T_0 can be observed and showed a higher ionic conductivity. In the case of L5C1, the low ionic conductivity was resulted from the low concentration of charge carrying ions. On the other hand, the ionic conductivity of L15C1 decreased with the increasing concentration of lithium salt. This is because the high concentration of lithium salts promote transient crosslinkers between the PEG chains[55] and reduce the mobility of PEG. It can be concluded that applying appropriate amount of lithium salt as well as substituting hydroxyl groups of CDs are important for improving

the ionic conductivity of polyrotaxane based SPE.It can be concluded that applying appropriate amount of lithium salt as well as substituting hydroxyl groups of CDs are important for improving the ionic conductivity of polyrotaxane based SPE. The discussion result was summarized in Figure 20.

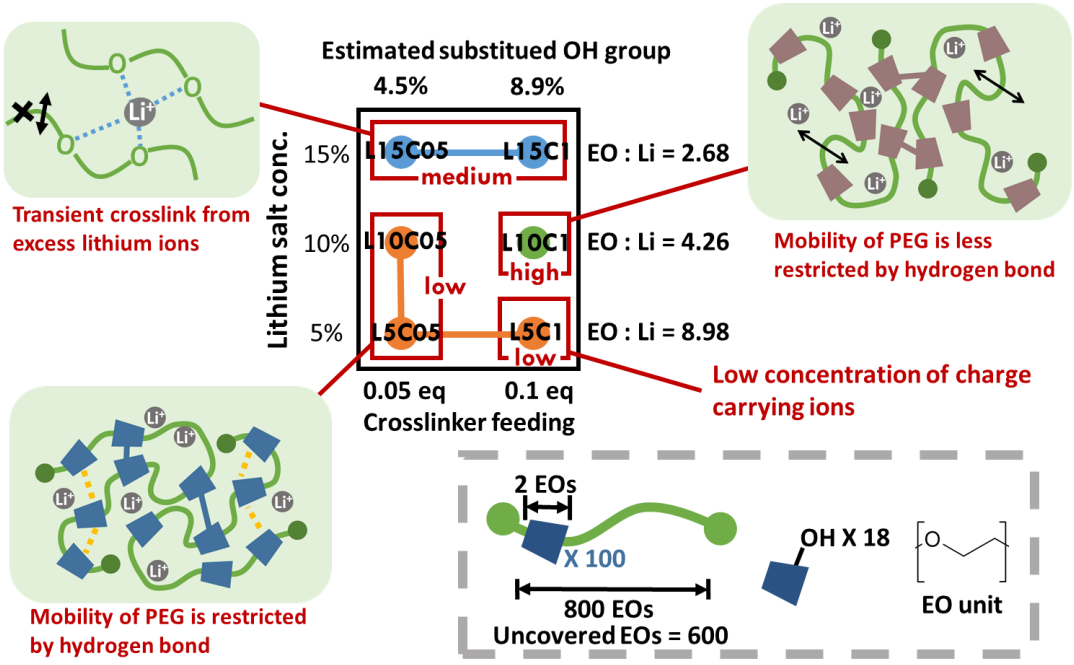

Figure 20. The proposed model of polyrotaxane based SPE

From the analysis of the experiment, we found out that the low ionic conductivity was the result of the hydrogen bond between CDs that restricts the mobility of PEG chain. Reducing the hydrogen bonding will be a good direction toward higher ionic conductivity. So, we were trying to load more HMDI crosslinkers to mask the hydroxyl groups on CDs to enhance the ionic conductivity. Figure 21 shows the ionic conductivity of PR based SPE with different loading of HMDI crosslinker. We push the loading of HMDI crosslinker upto 25 wt%, but the ionic conductivity becomes even lower than the SPE with 10 wt% HMDI crosslinker. The decrease in ionic conductivity was probably resulted from the excess crosslinker that makes the CDs aggregated.

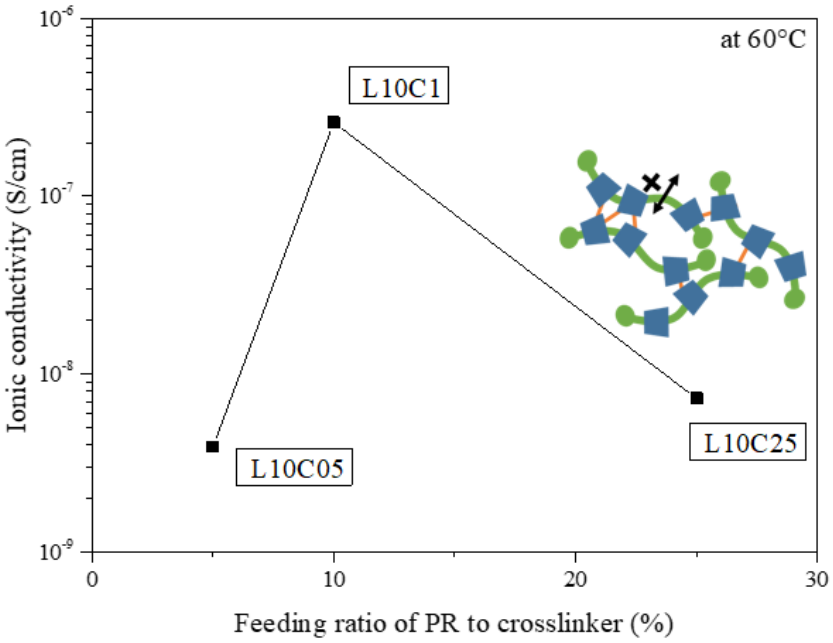

Figure 21. The Arrehnius plot of polyrotaxan based SPE in different crosslinker ratio and the proposed model of polyrotaxane with excess crosslinker

4.3 Functionalization of PR based SPE

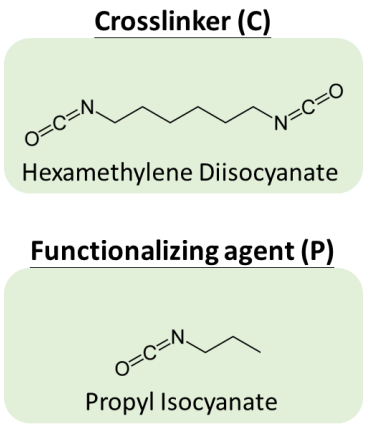

Figure 22. The Chemical structure of crosslinker and functionalizing agent used in SPE

Table 3. The composition and thermal data of modified polyrotaxane based SPE

sample	wt% $_{LiClO4}$ (%)	PR:HMDI:PI	T_m (°C)	Xc $_{PEG}$ (%)	Xc $_{PR}$ (%)
PEG	0	--	65.4	100	--
PR	0	--	56.9	3.1	100
L10C05	10	10:0.5 (no PI)	53	0.16	5.1
L10C05P2	10	10:0.5:2	53.7	0.31	10.2
L10C05P5	10	10:0.5:5	46.5	0.03	0.99

T_m = melting temperature

Xc $_{PEG}$= crystallinity index of PEG = $\frac{\Delta H_m}{\Delta H_{mPEG}}$ Xc $_{PR}$= crystallinity index of PR = $\frac{\Delta H_m}{\Delta H_{mPR}}$

ΔH_m = enthalpy of sample obtained from DSC

$\Delta H_{m\ PEG}$ = enthalpy of PEG (MW=35,000) obtained from DSC

$\Delta H_{m\ PR}$ = enthalpy of PR (MW=135,000) obtained from DSC

From the previous part, we found out that HMDI crosslinkers cannot be added more to block hydroxyl groups on CDs or the ionic conductivity will be decreased. Propyl isocyanate (PI) which shares the similar chemical structure with HMDI crosslinker as shown in **Figure 22** was used as a functionalizing agent that is able to mask the hydroxyl groups on CDs but not crosslink the polyrotaxane. The naming and the composition of these modified SPEs with different amount of propyl isocyanate, low HMDI crosslinker feeding ratio and 10 wt% lithium salts can be found in **Table 3**.

Table 4. The mechanical properties of PR based SPE with and without modification of PI

sample	Ultimate tensile strength (MPa)	Young's modulus (MPa)	Elongation at break (%)
L10C05	21.8	756	17.5
L10C05P2	16.6	570	191
L10C05P5	20.6	2385	0.93

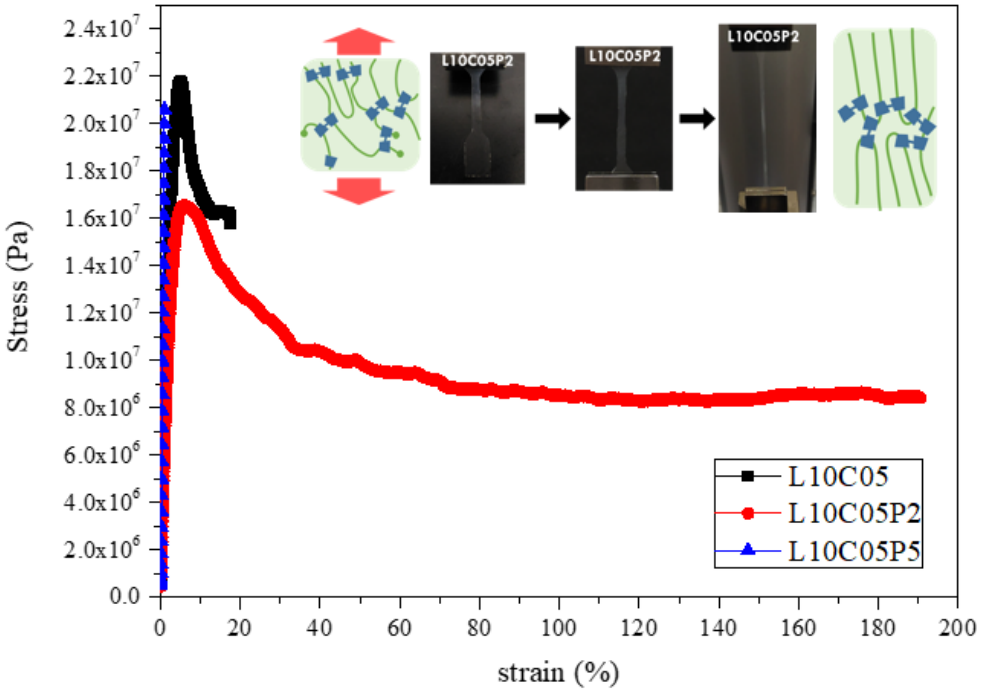

Figure 23. The stress strain curve and the photos of polyrotaxane based SPE with and without modification of PI

The mechanical properties of the unmodified and modified SPEs are summarized in **Table 4**. L10C05 which was not modified by PI showed a very high tensile strength over 20 MPa and had nearly 20% strain at break. If the SPE was modified by moderate amount of PI as L10C05P2, the tensile strength was lowered to 16.6 MPa but showed an impressively high elongation up to approximately 200% strain contributed by the pulley-effect of the slide-ring material[33] as shown in **Figure 23**. During the stretching, the specimen was gradually whitened till break which is most likely coming from the strain-induced crystallization of PEG. In L10C05P5, the amount of PI was further increased and the tensile strength of the specimen was returned to 20 MPa and showed a huge increase in Young's modulus but the strain at break decrease down to 1%.

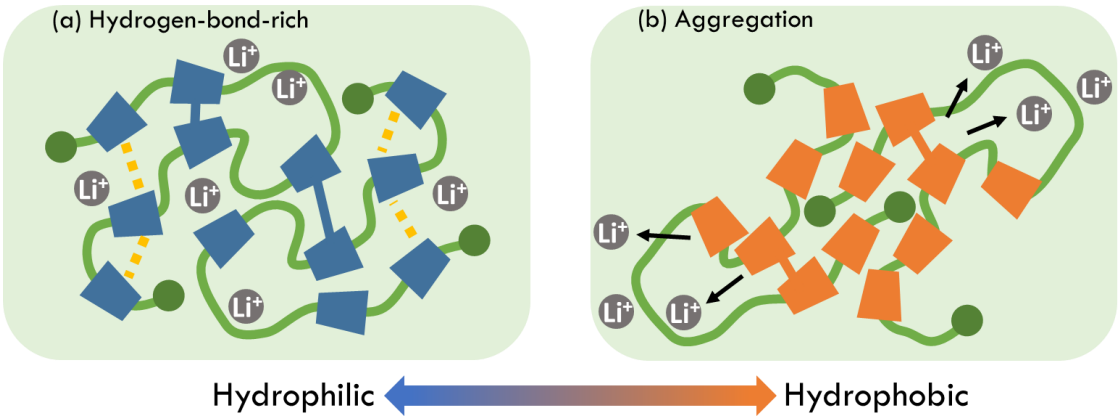

Figure 24. The proposed model of polyrotaxane based SPE with and without the modification of propyl isocyanate. (a) The CDs are not modified and the SPE is suffered from strong hydrogen bonding. (b) The CDs are excessively modified that leads to an aggregation

In the previous work of our group[56], the behavior of slide ring gel in poor and good solvent was discussed and proved. The slide-ring gel with good solvent, the polymer chain can move freely through the crosslink. On the other hand, when the slide-ring gel is immersed in poor solvent for CDs, the CD crosslinks aggregate, and restrict the movement of polymer chain. Similarly, PI-modified hydrophobic CDs in the SPE may

aggregate to avoid the contact with surrounding ions as shown in **Figure 24**. If the polyrotaxane was not modified, the strong hydrogen bonding provides a high tensile strength but allows only a small deformation before the SPE break as in L10C05. After a moderate addition of PI, the hydrogen bond is reduced and the decrease in tensile strength can also be observed. The high elongation of L10C05P2 is most likely coming from the effective slide-ring movement of the less restricted CDs. If PI is further increased (L10C05P5), the CDs become very hydrophobic and aggregate due to the strong CD-CD attractive hydrophobic interaction in an ionic surrounding media. To further investigate the aggregation of polyrotaxane caused by the modification of PI, small angle X-ray scattering (SAXS) was performed and the result is shown in **Figure 25**. After the functionalization of PI, the polyrotaxane based SPE shows significantly increased scattering intensity at low wave number. Such scattering suggests large aggregation with a broad size distribution compared with the unmodified SPE, which is compatible with the model we proposed.

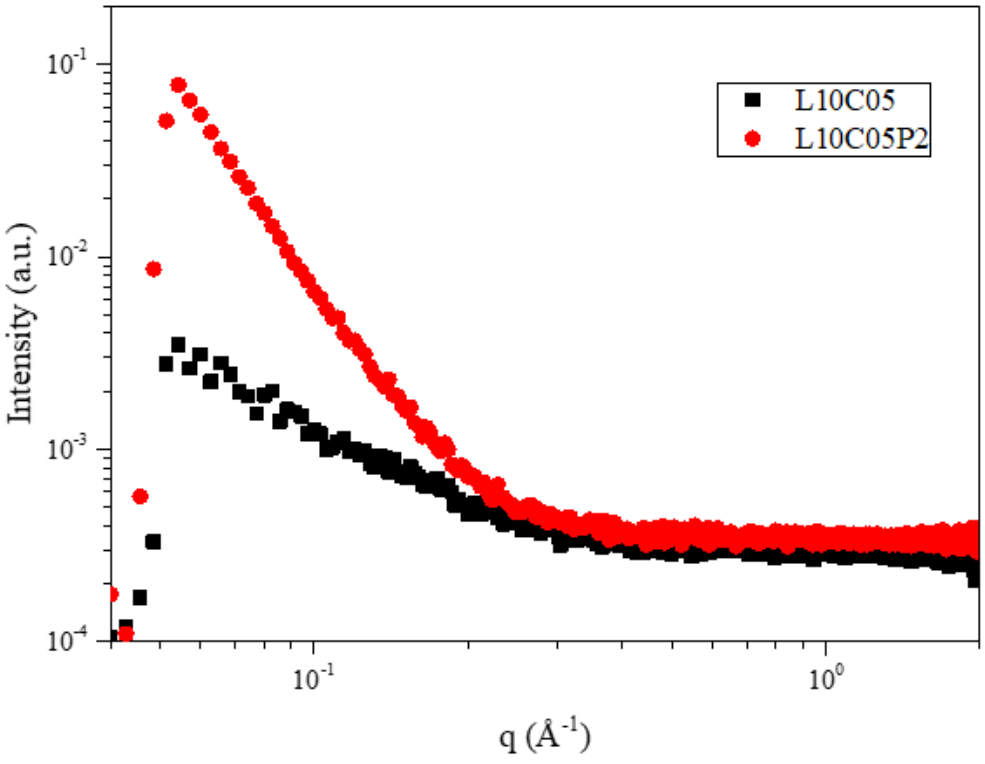

Figure 25. The SAXS data of polyrotaxane based SPE before and after modification of PI

Figure 26 is the Arrhenius plot of the SPEs with and without modification of PI. After a moderate addition of PI, by which the hydroxyl groups on CDs were substituted but not crosskinked, the ionic conductivity of L10C05P2 remarkably increased. But if we further increase the amount of PI, the ionic conductivity of L10C05P5 dropped down again. The ionic conductivity of the modified PR based SPE can also be fitted by the combination of Arrhenius equation and VTF equation as above and the parameters are summarized in **Table 3**. All the three samples share similar "A" parameter since all the samples have 10wt% lithium salt. In L10C05P2, the modified SPE showed a lowest activation energy which suggests that polymer chain of PEG was less restricted by the CDs and crosslinks and showed a higher mobility in SPE and leads to the higher ionic conductivity. On the other hand, if the SPE was modified too much, the activation energy was highly increased even the T_0 was reduced and caused low ionic conductivity. It just meets our assumption that the PEG chains are restricted by the aggregation of CDs rather than the hydrogen bonds.

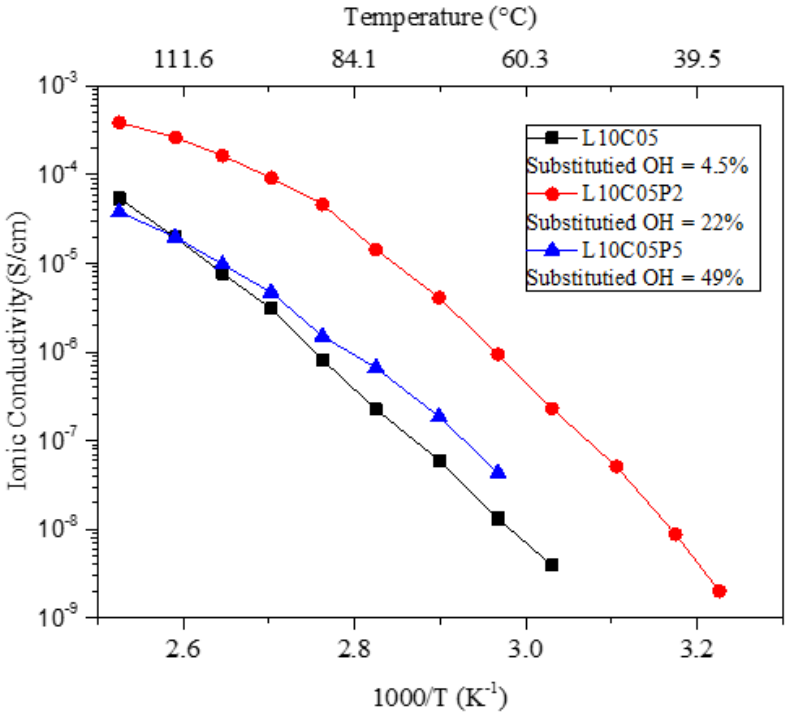

Figure 26. The Arrhenius plot of PI modified SPEs

To further investigate the relationship between mechanical strength and ionic conductivity, DMA was performed and the result is shown in **Figure 27**. In the DMA thermogram, L10C05 and L10C05P2 shows a similar feature of glass transition but L10C05 which is suffered from intensive hydrogen bonding is stiffer than the PI-modified L10C05P2. On the other hand, the stiffness of L10C05P5 that majorly comes from the aggregation of CDs and crosslinks but not hydrogen bond was higher than the other SPEs and the storage modulus dramatically decreases near 60°C which is the melting temperature of PEG. We also denoted the Tc derived from the Arrhenius plot on the DMA thermogram. The transition from Arrhenius behavior to VTF behavior suggests that the PEG chains are able to perform segmental motion and we can observe that a similar storage modulus were shared in T_c of each sample.

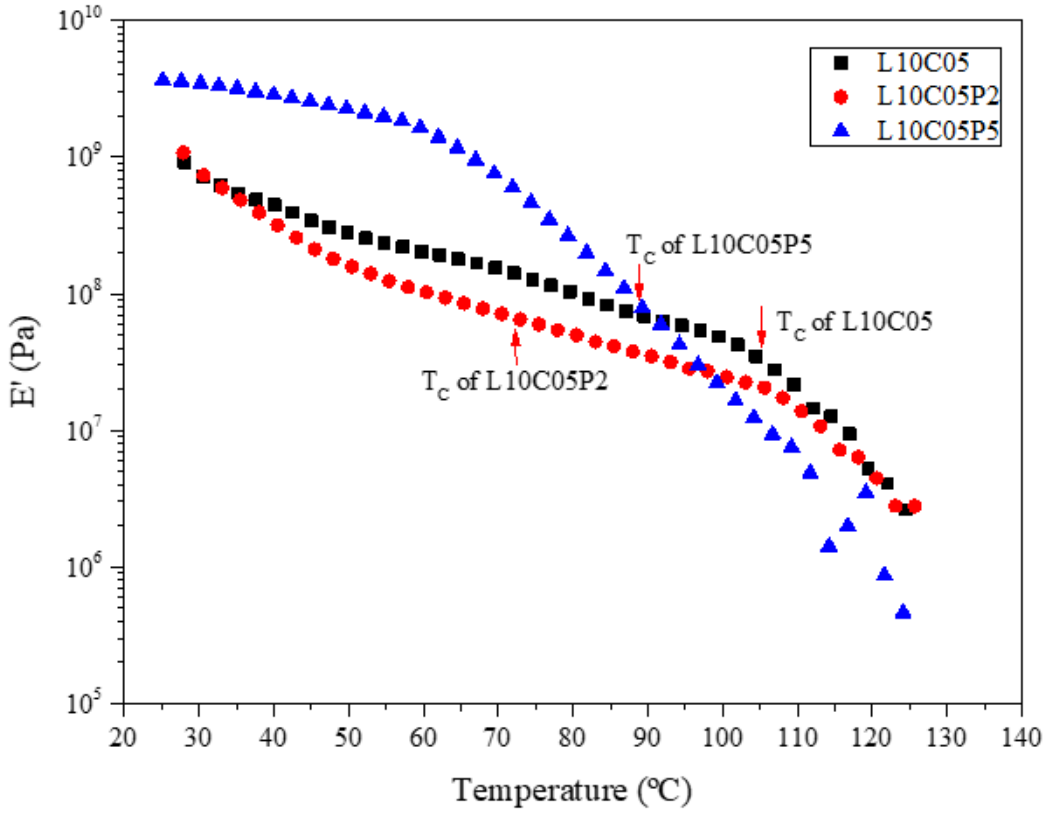

Figure 27. The DMA result and the Arrhenius plot of PI modified SPEs

4.4 Summary

In this section, solid polymer electrolyte based on polyrotaxne that composed of PEG and CDs were successfully prepared with $LiClO_4$ and HMDI crosslinker. The ionic conductivity was highly affected by the concentration of lithium salt and the strong hydrogen bonding between CD crosslinks that restricts the mobility of PEG chain. To eliminate the effect from hydrogen bonding, PI was applied as functionalizing agent. The L10C05P2 with moderate lithium salt and functionalizing agent shows a high elongation up to 200% strain and the ionic conductivity of 10^7 S/cm at 60°C. The high elongation supports the existence of noncovalent "mobile crosslink." And the concept shows a good potential in the future development of SPE if we could find an appropriate functionalizing agent which can prevent the hydrogen bonding as well as aggregation of CDs.

Chapter 5. Polyrotaxane based SPE with macromolecular crosslinker

5.1 Motivation and research scope

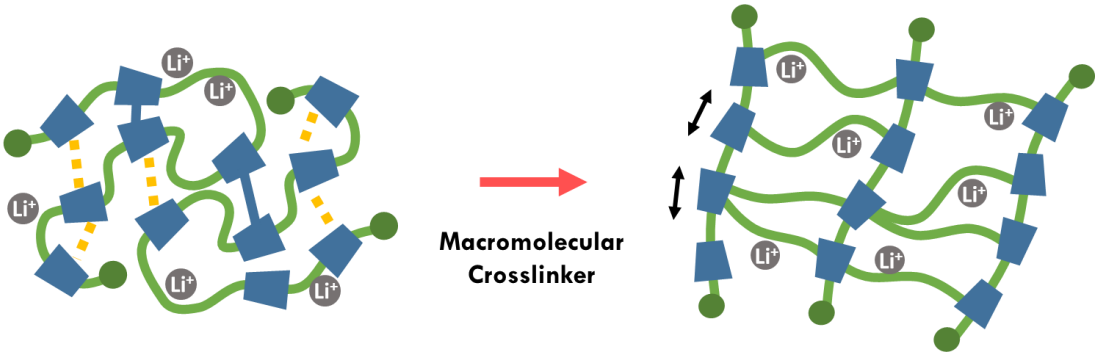

Figure 28. The proposed model of PR based SPE with macromolecular crosslinker

In the previous chapter, we found out that the polyrotaxane based SPE was suffering from the low ionic conductivity because of hydrogen bond and the aggregation of CDs and crosslinks. In order to enhance the ionic conductivity, reduction of hydrogen bond and dispersion of CDs are important. And we also know that the aggregation of CDs is coming from the differenc hydrophobicity between CDs and PEG. Therefore, adding a hydrophilic macromolecular crosslinker may be a good choice to prevent the CDs from either hydrogen bonding and aggregation as shown in **Figure 28**. The hydrophilic macromolecular crosslinker may work as a spacer between the CDs and prevent the

aggregation or hydrogen bond without losing the slide-ring effect and mechanical strength. Furthermore, the hydrophilic macromolecular crosslinker itself can be involved in the conduction of lithium ion[57] and thus the ionic conductivity can be enhanced.

5.2 Polyrotaxane based SPE with PEGDE as crosslinker

5.2.1 Preparation of PR based SPE with PEGDE

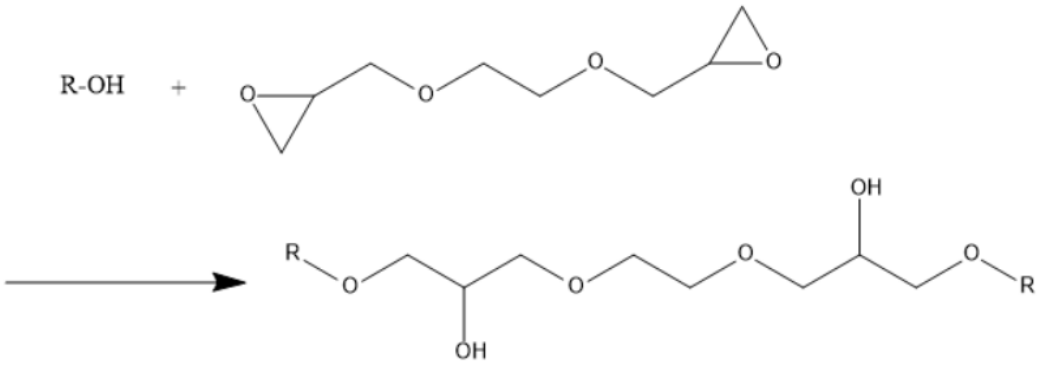

Figure 29. The crosslink reaction of PR with EGDE

The crosslink reaction was shown in **Figure 29**. HAPR and battery grade $LiClO_4$ were first dissolved in super dehydrated DMF. Then EGDE or PEGDE (MW=500) were added to the solution under vigorously stirring at 60°C for 12 hours. The mixed solution was then poured into a Teflon petri dish and dried at 80°C for 12 hours to obtain the SPE membrane. The membrane was then evacuated at 80 °C for another 24 hours to remove the residual solvent and then heated upto the highest measuring temperature (150 °C) for 30 minutes to ensure no side reaction will occur during the electrochemical measurements. The thickness of the membrane is approximately 250 μm. All the chemicals were used as received.

5.2.2 The property of PR based SPE with PEGDE

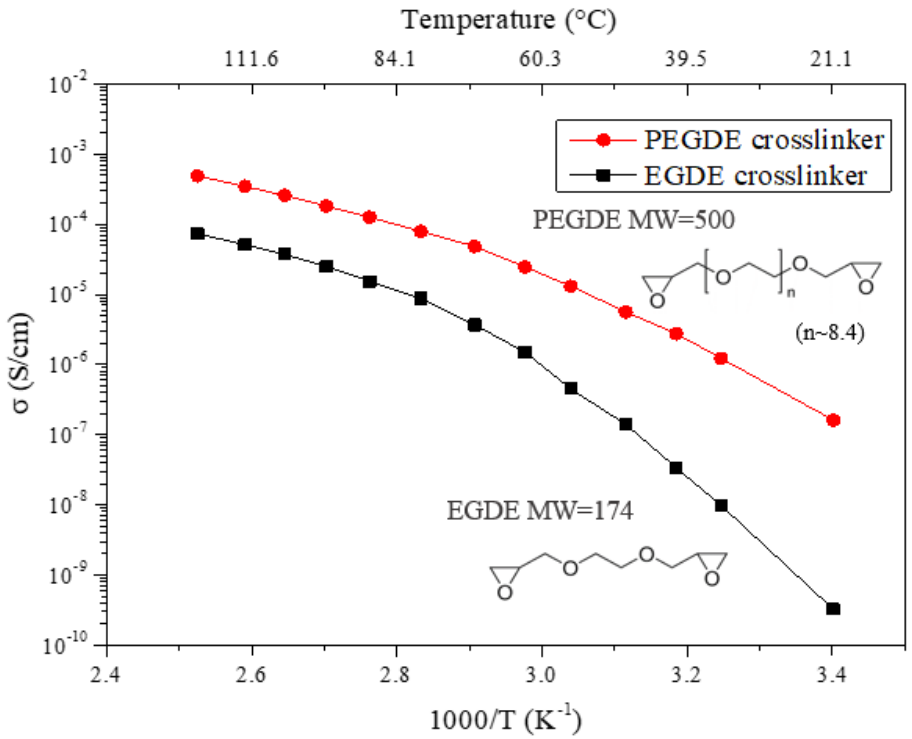

Figure 30. The ionic conductivity of PR with EGDE and PEGDE crosslinker

Figure 30 shows the Arrehinus plot of the SPE prepared with short EGDE and macromolecular PEGDE crosslinker. EGDE has been reported as a crosslinker for polyrotaxane[58] and the macromolecular crosslinker PEGDE with same chemical structure and di-epoxy functional group is commercially available which makes it a perfect crosslinker for our experiment. The ratio of hydroxyl group of polyrotaxane to epoxy group of crosslinker is the same in SPE with both EGDE and PEGDE crosslinker. The polyrotaxane based SPE with short EGDE crosslinker that contains only one ethylene oxide (EO) unit shows a very low ionic conductivity in the order of 10^{-9} S/cm at room temperature. On the other hand, the SPE crosslinked by PEGDE that contains approximately 8.4 EO unit (molecular weight = 500) shows a high ionic conductivity in the order of 10^{-6} S/cm at room temperature. The ionic conductivity has an impressive three-oreder-high enhancement with the use of macromolecular crosslinker.

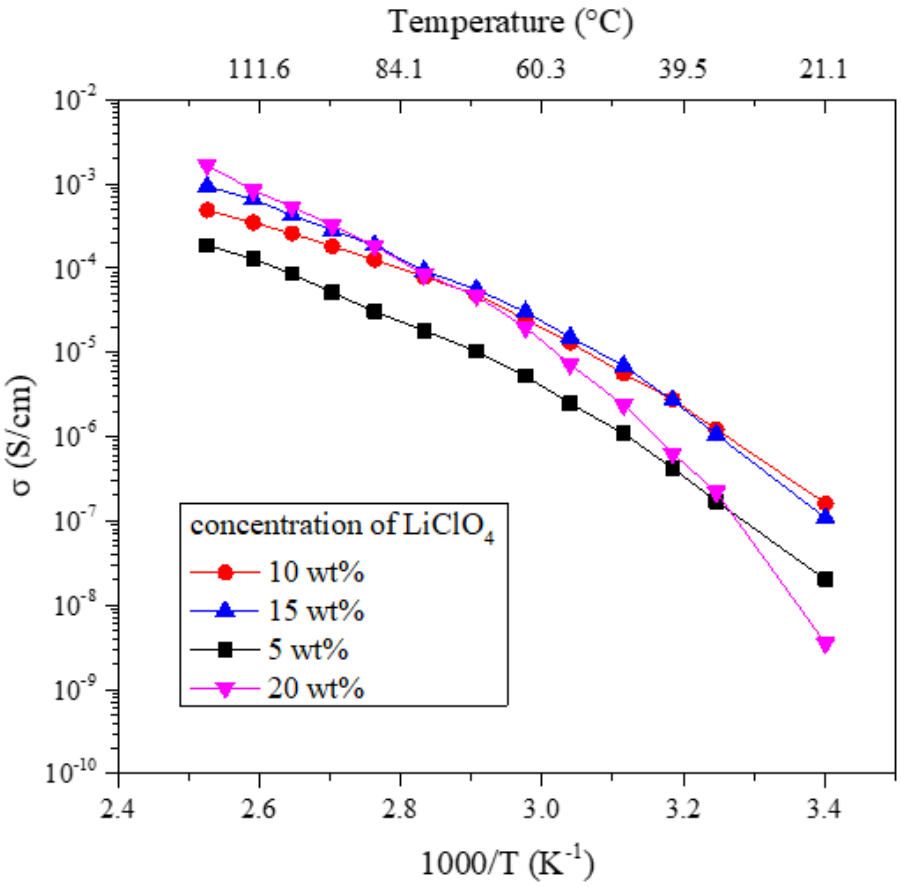

Figure 31. Polyrotaxane based SPE with macromolecular crosslinker in different lithium salt concentration

The ionic conductivity of PR based SPEs crosslinked by PEGDE with various concentration of lithium salt were also studied and shown in Figure 31. The SPE with only 5wt% lithium salt shows an extremely low ionic conductivity which is probably caused from the lack of charge carrying ions. If we further increase the amount of lithium salts, the ionic conductivity at room temperature was increased in the first place and then decreased while the concentration was further increased. The ionic conductivity of SPE with 20 wt% of lithium salts was even lower than the SPE with 5 wt% lithium salt. As we have mentioned before, the phenomenon is because the excess lithium salts formed transient crosslinkers between the PEG chains [16] and reduce the mobility of PEG.

(a) **(b)**

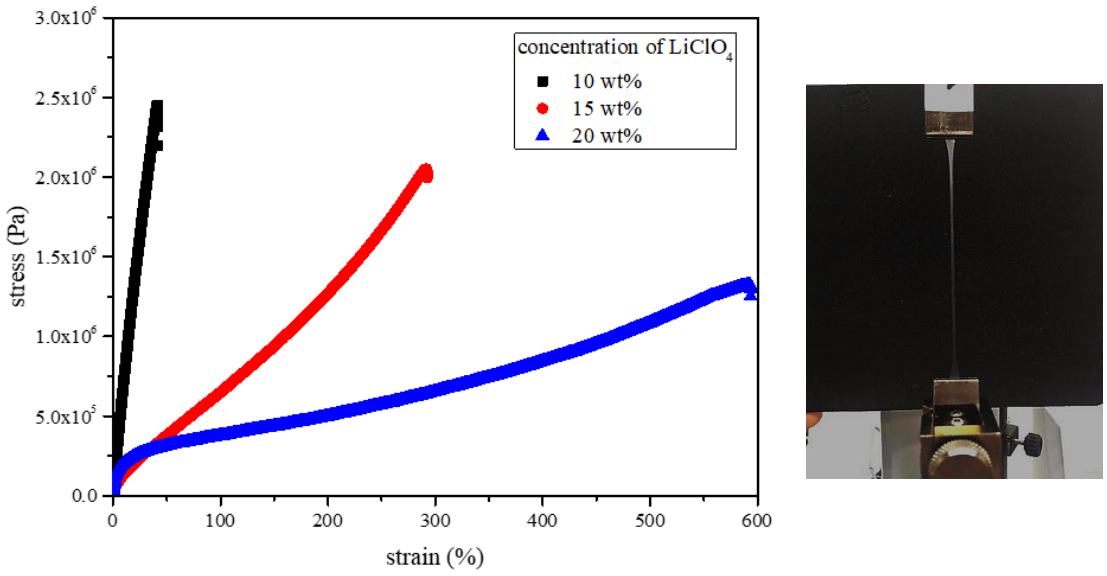

Figure 32. (a) The stress-strian curve of SPE with macromolecular crosslinker in different lithium salt concentration (b) the photo of polyrotaxane based SPE crosslinked by PEGDE with 20 wt% LiClO4

Moreover, the mechanical property of the SPE crosslinked by PEGDE has a large difference with the SPE prepared from short crosslinker. The stress strain curve of SPE crosslinked by PEGDE with various concentration of $LiClO_4$ was shown in **Figure 32**. The ultimate tensile strength of SPE crosslinked with PEGDE was about 1 to 2 Mega pascal which is an order lower than the SPE with short crosslinker as shown in **Figure 23**. And unlike the brittle polyrotaxane based SPE in the previousr part, the polyrotaxane based SPE crosslinked by macromlecular PEGDE is more flexible and soft. As we have mentioned before, the stiffness majorly coming from either the aggregation of CDs or the hydrogen bond. So, the result just meets our expectation that the use of macromolecular crosslinker can reduce the hydrogen bonding and prevent the aggregation of CDs and crosslinks as shown in Figure 28.

5.3 Polyrotaxane based SPE with two-step reaction

5.3.1 Two-step synthesis

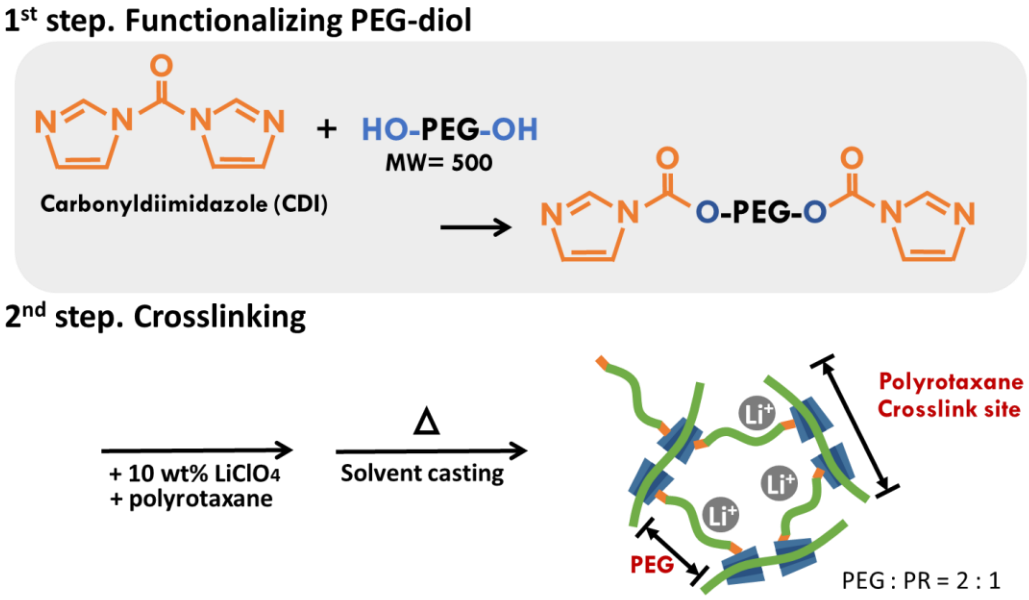

Figure 33. The two-step synthesis of PR bases SPE with macromolecular crosslinker

The impressive enhancement in ionic conductivity with the use of macromolecular crosslinker in PR based SPE has attracted our attention. Increasing the concentration of flexible macromolecular PEG crosslinker in the PR based SPE seems showing an advange to enhance the ionic conductivity. However, the reactivity between epoxy groups of PEGDE and hydroxyl groups of CDs is very low without catalyst. If we're trying to load more PEG crosslinker to the SPE, another crosslink reaction with higher reactivity is required since the catalyst may affect the ionic conductivity and the chemical stability of SPE. **Figure 33** shows the two-step crosslink reaction we proposed. The two-step reaction is commonly used in the preparation of polyurethane. A prepolymer is formed in the first step by blending the "polyol" with di-isocyanate and this prepolymer was then blended with a hard chain-extending-agent to form the polyurethane with alternating hard and soft segements[59]. In this research, a similar reaction was performed, but the synthesized SPE will be a network structure we have mentioned in **Chapter 2.1.2** instead of a linear polymer chain like polyurehtane. In the first step, PEG-diol (1 eq, MW=1000) was reacted with CDI (2.1 eq) under argon and vigorous stirring in DMF for 24 hours at 60°C to form the macromolecular crosslinker. And then the obtained macromolecular crosslinker was

injected into the DMF solution of polyrotaxane and $LiClO_4$. The mixed solution was then poured into a Teflon petri dish and dried at 80°C for 12 hours to obtain the SPE membrane. The membrane was then evacuated at 80°C for another 24 hours to remove the residual solvent and then heated upto the highest measuring temperature (150 °C) for 30 minutes to ensure no side reaction will occur during the electrochemical measurements. The thickness of the membrane is approximately 200 μm and shows good flexibility. All the chemicals were used as received.

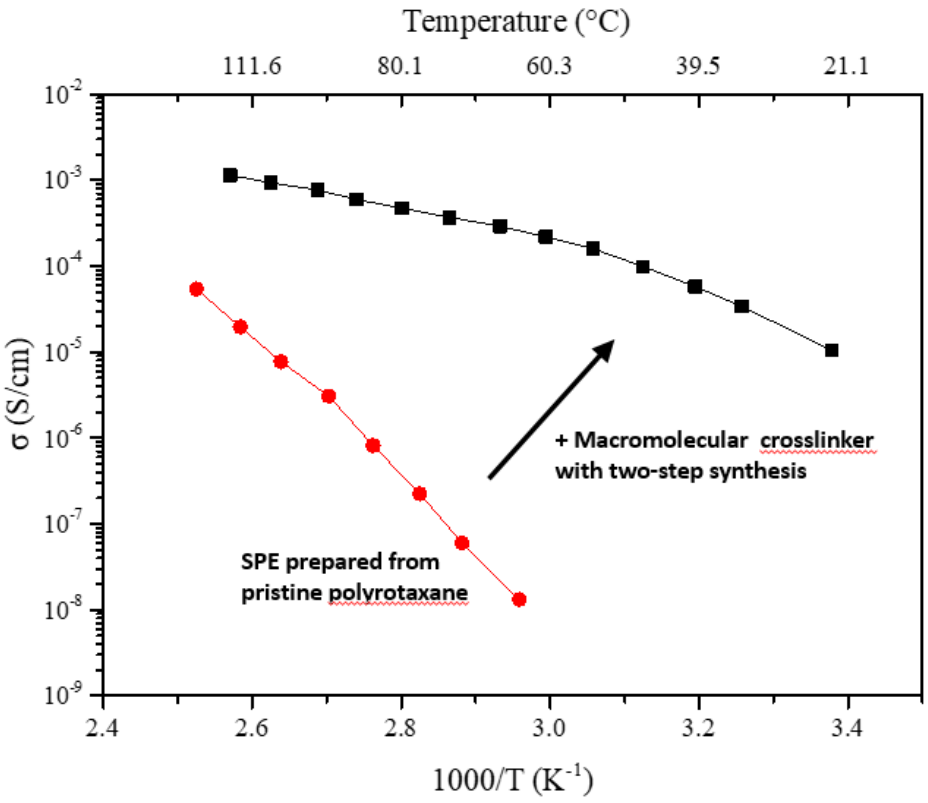

Figure 34. The ionic conductivity of SPE prepared with pristine polyrotaxane and the two-step synthesis

Figure 34 shows the ionic conductivity of SPE prepared with pristine polyrotaxane and from the two-step synthetic method. The ionic conductivity was higly enhanced by using the two-step process with PEG crosslinker. And the loading of PEG crosslinker was also enhanced. The ionic conductivity of the SPE can be as high as 10^{-5} S/cm at room temperature. The SPE shows a high potential in the fabrication of lithium battery.

5.3.2 Comparision with cellulose

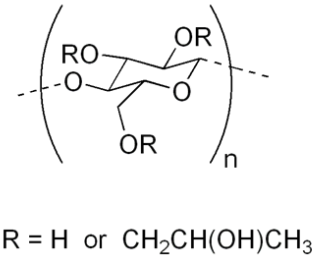

Figure 35. The chemical structure of hydroxylpropyl cellulose

With the success of using two-step reaction to promote the loading of macromolecular crosslinker in SPE, we are trying to compare the polyrotaxane based SPE with other materials using the same process. Hydroxypropyl cellulose is a cellulosic material with good soubility in various solvent and shares a similar chemical structure with polyrotaxane as shown in **Figure 35**. The cellulosic material is also a commonly used material in the preparation of SPE since it can enhance the mechanical strength[60], thermal and chemical stability of SPE[61]. However, the stiffness of the cellulose has restrict its performance and the cellulose is usually used with other softer material in the fabrication of SPE[62]. The Hydroxylpropyl cellulose we used in this research shares same average glucose unit with polyrotaxane in one macromolecule.

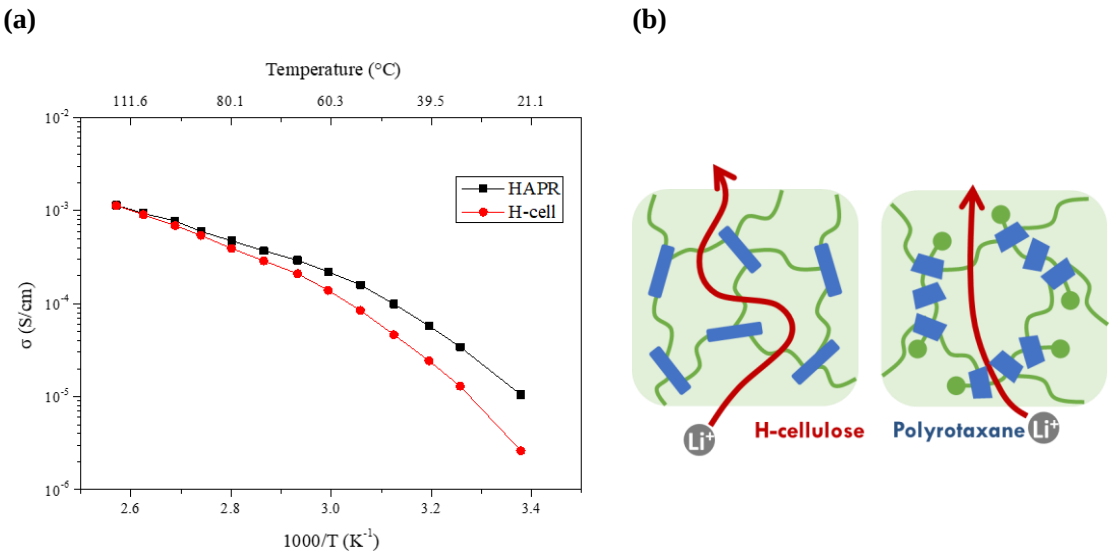

Figure 36. (a) The Arrehnius plot of SPE based on polyrtaxane and cellulose and (b) the proposed model of ion conduction in SPEs

Figure 36 (a) shows the ionic conductivity of SPE prepared from polyrotaxane and cellulose via two-step synthesis. We can observe that the ionic conductivity of polyrotaxane based SPE was one order higher than the one based on cellulose at room temperature and the ionic conductivity becomes almost the same upon 100°C. The difference in ionic conductivity is probably coming from the difference in the mobility of polymer chain. Polyrotaxane is much more flexible than the cellulose because of its topological structure and the axis PEG chain can also contribute to the ionic conduction as shown in **Figure 36** (b). At high temperature, the chain mobility of both materials is enhanced to a rather high level and the difference in ionic conductivity is not that obvious.

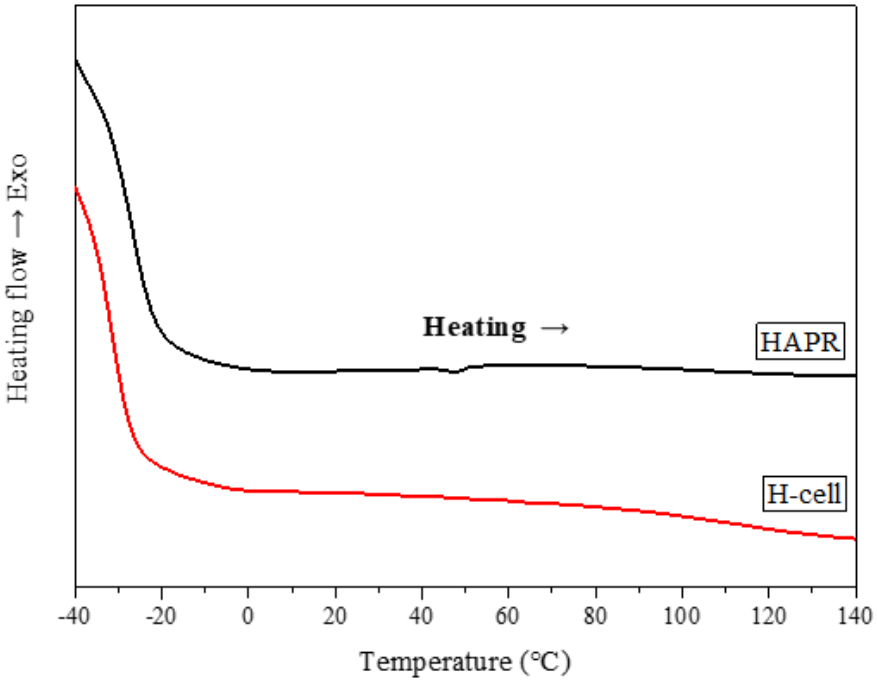

Figure 37. The DSC thermogram of SPE based on polyrtaxane and cellulose

Figure 37 is the DSC thermogram of the SPE based on polyrotaxane and cellulose via two-step reaction. We can observe that both of the SPE has a very low Tg at around -20°C. It does not like the polyrtaxane base SPE we prepared in **chapter 4.2** which shows a broad T_g ended at around 100°C which arises from the hydrogen bond of polyrotaxane. The introduction of macromolecular crosslinker do reduce the hydrogen bond and enhance the ionic conductivity as our expectation. And the mechanical property is also recorded with DMA as shown in **Figure 38**. The DMA data suggests that the mechanical strength of cellulose based SPE was highly affected by temperature, which is not a good property in lithium ion battery since the temperature changed frequently while the battery is working. On the other hand, the mechanical strength of polyrotaxane based SPE is independent with the temperature change below 100°C. It's a rare property that is likely resulted from the slide-ring effect of polyrotaxane. And it also shows a great advantage in the fabrication of SPE that can prevent the break of SPE membrane in a high and changing working temperature.

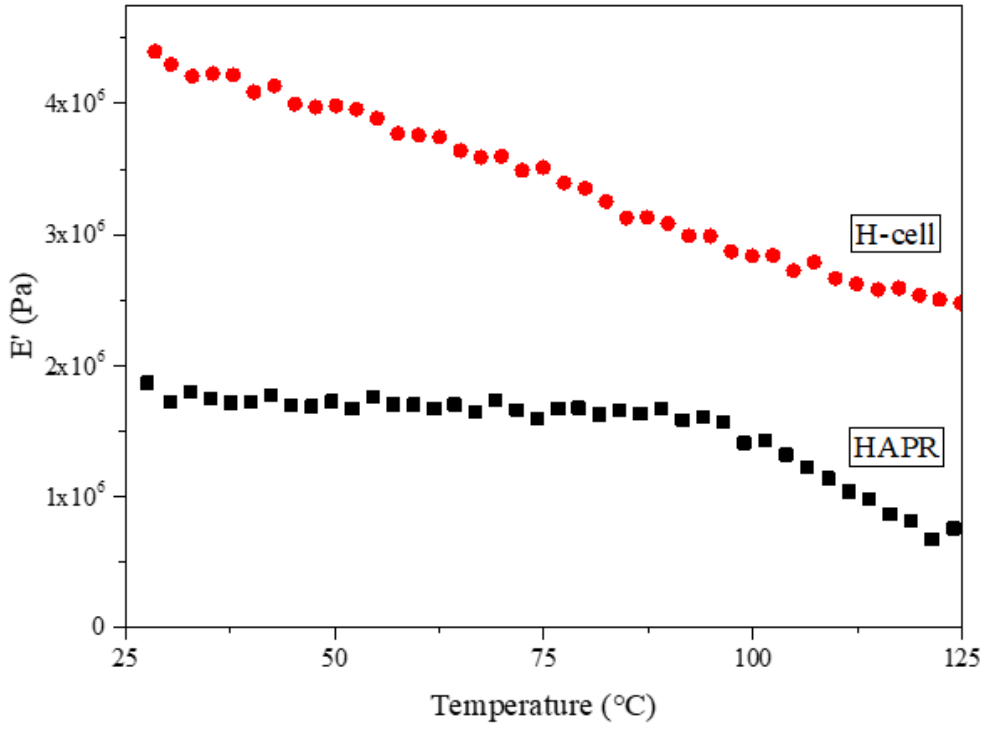

Figure 38. The DMA result of SPE based on polyrtaxane and cellulose

5.4 Summary

In this section, we used two kinds of macromolecular crosslinking reaction to make the SPE. The SPE based on PEGDE shows a great enhancement than the SPE with short EGDE crosslinker which proved that the macromolecluar crosslinker do prevent the hydrogen bonding and aggregation of CD. Two-step reaction was used to enhance the loading of macromolecular crosslinker. The ionic conductivity of polyrotaxane based SPE prepared form two-step reaction can be as high as 10^{-5} S/cm at room temperature. The unique mechanical property that the strength of SPE was nearly not affected by the changing of temperature also shows a great advantage in the fabrication of SPE in lithium ion battery.

Chapter 6. Single ion conducting SPE based on polyrotaxane

6.1 Motivation and research scope

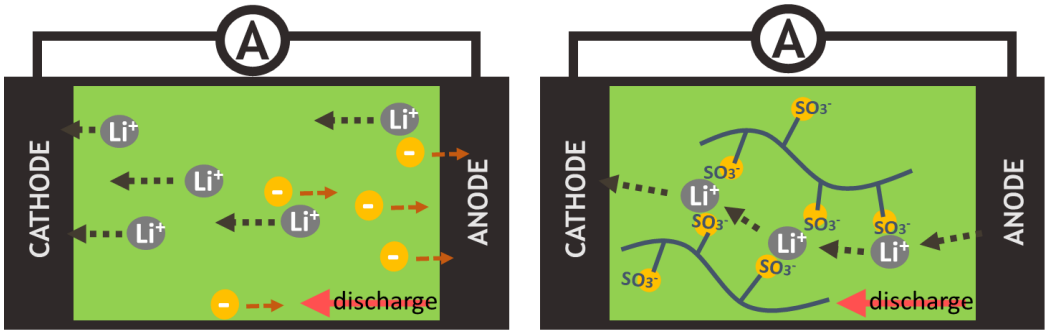

Figure 39. (a) The ion transportation in normal lithium battery and (b) the ion transportation in single ion conducter

As we have mentioned in **Chapter 2.1.3**, the design of single ion conductor can prevent the lithium battery suffering from concentration gradient of the counter ions and improve the battery efficiency as shown in **Figure 39**. However, the strong "ionic crosslink" has restrict the mobility of polymer chains and led to the low ionic conductivity in most of the single ion conducting SPE as shown in **Figure 40 (a)**. In order to enhance the ionic conductivity, people usually introduce a flexible polymer segement to the ion-bearing polymer. In this part, we are providing a new strategy to enhance both the ionic conductivity and mechanical property of single ion conducting SPE by using the ionized polyrotaxane. The ionized cyclodextrin is expected to work as the crosslink as well as the source of lithium ion and where the axis PEG can provide the flexibility and contribute to the conduction of lithium ion as shown in **Figure 40 (b)**. The single ion conducting SPE based on polyrotaxane is expected to show a higher ionic conductivity and a better ductility than the conventional single ion conducting SPE with the unique chemical structure of polyrotaxane.

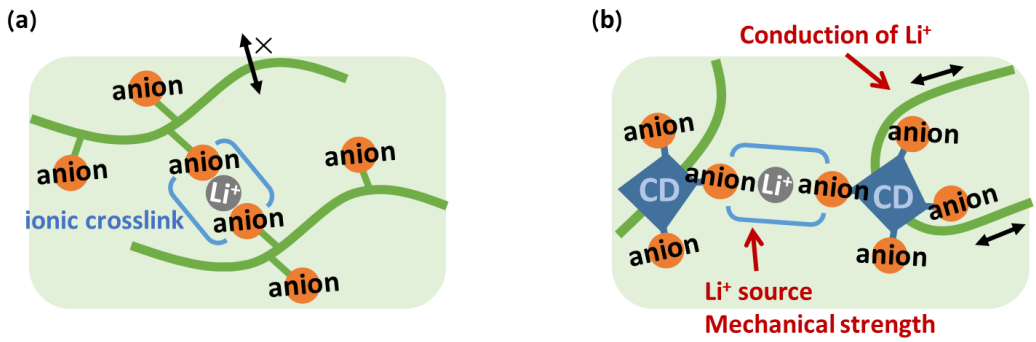

Figure 40. (a)Normal single ion conducting SPE and (b) single ion conducting SPE based on polyrotaxane with ionic group

6.2 Synthesis of ionized polyrotaxane

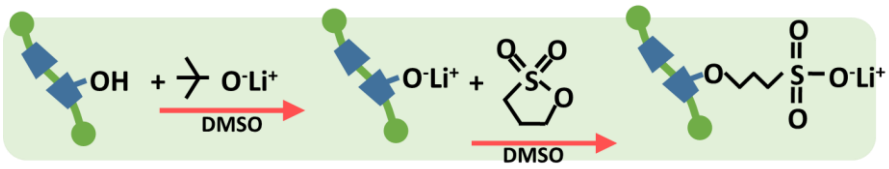

Figure 41. The ionization of polyrotaxane

The synthesis route was shown in **Figure 41**. HAPR were first dissolved in super dehydrated DMSO. Then LiOH was added to the solution under vigorously stirring for 12 hours in argon dropwisely in order to prevent the gelation. 1,3-Propane sultone was injected slowly to the flask in iced bath under vigorously stirring and followed by stirring for 12 hours at 80°C. The solution was purified by dialysis and frozen dried to remove water and the residue reactants. The sample was made by hot pressing the ionized polyrotaxane and the thickness is approximately 300 μm.

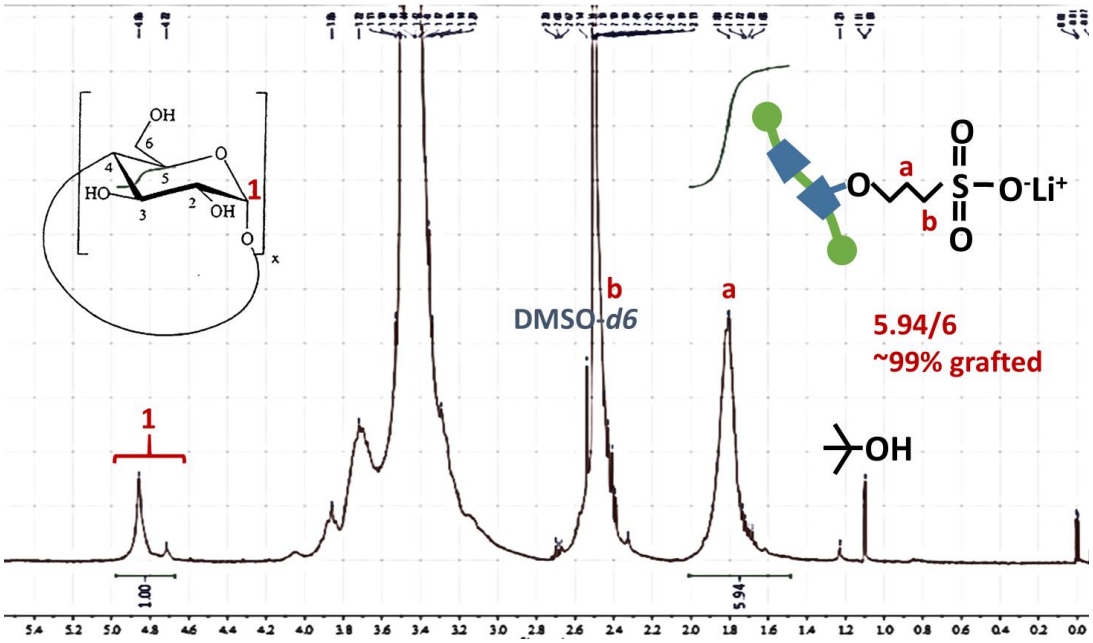

Figure 42. NMR result of ionized polyrotaxane

1H NMR test was held to examine the functionalization of ionic group. From **Figure 42**, we can observe a broad single peak at 1.8 ppm and a peak overlapped with DMSO-*d6* peak at 2.5 ppm after functionalization of polyrotaxane. The two peaks were confirmed as the peak of sulfonated groups[63]. And by comparing the integral of "1" on cyclodextrin which locates at 5.0 ppm to 4.6 ppm to the "a" peak of the sulfonated functional group at 1.8 ppm, we can calculate the functionalization ratio of the polyrtoaxane which is approximately 99%.

6.3 The performance of ionized PR based SPE

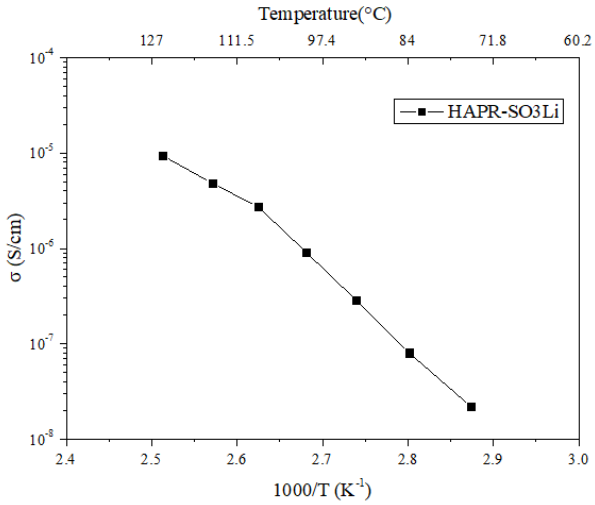

Figure 43. The ionic conductivity of polyrotaxane based single ion conducting SPE

Table 5. The solubility change after ionization of HAPR

	Solubility	
	HAPR	+SO_3Li*
Water	good	Very good
DMSO	good	poor
DMF	good	insoluble

*After functionalization

The SPE is much more brittle than the normal PR based SPE and is in the color of yellow. The solubility was also changed after functionalization as shown in **Table 5**. The ionized polyrotaxane becomes insoluble in DMF but very easy to be dissolved in water. The ionic conductivity of the hot-pressed ionized polyrotaxane is pretty low which is in the order of 10^{-7} at around 70°C as shown in **Figure 43**. It is about one order lower than the polyrotaxane/LiClO4 system in the previous section at the same temperature.

6.4 Single ion conducting SPE prepared from polyrotaxane graft copolymer

(a)

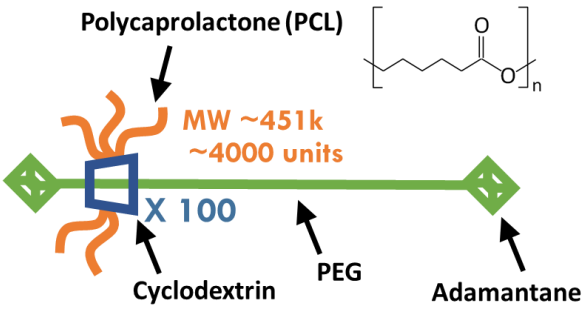

(b)

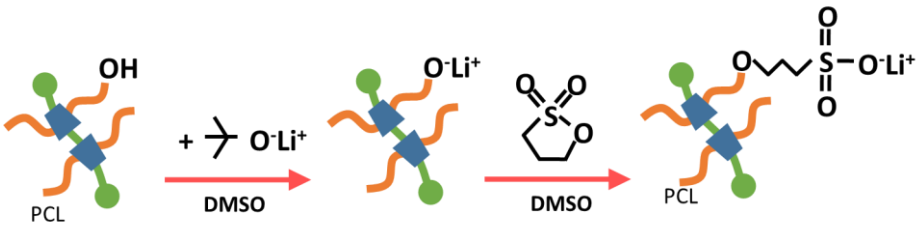

Figure 44. (a) The model of graft polyrotaxane, "PCLPR" and (b) The synthesis of ionized PCLPR

Since the ionic conductivity of ionized polyrotaxane based SPE is not as high as we expected, we came up with another strategy of using "graft polyrotaxane" to make the SPE. PCLPR is the polyrotaxane grafted with PCL segements as shown in Figure 44 (a). The slide-ring material prepared from PCLPR is a elastomer that shows less strain-hardening than the material with conventional chemical crosslink[64]. Furthermore, PCL is a promising material for lithium ion conduction with good flexibility[65]. So, we were expecting that the ionic conductivity and the mechanical property can be enhanced by introducing a flexible ion conducting block between the polyrotaxane and the ionic functional group. The synthesis route is similar to the previous part as depicted in Figure 44 (b). The solubility was also changed after functionalization as shown in Table 6. The ionized graft polyrotaxane was orginally insoluble in water, but it becomed water-soluble after functionalization.

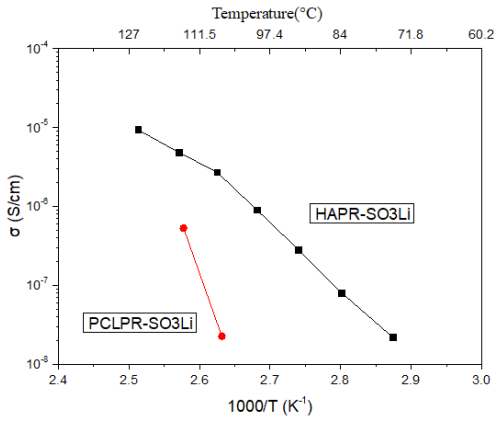

Figure 45. The ionic conductivity of ionized HAPR and PCLPR based SPE

Table 6. The solubility change aof PCLPR after functionalization

	Solubility	
	PCLPR	+SO_3Li*
Water	insoluble	poor
DMSO	good	good
DMF	insoluble	poor
THF	good	dispersed

*After functionalization

The ionic conductivity of the hot-pressed ionized graft polyrotaxane is shown in **Figure 45**. The ionic conductivity is even lower than the polyrotaxane based SPE without graft. And the graft polyrotaxane based SPE is as brittle as the one without graft. It seems like the introduction of a flexible block between the polyrotaxne and the ionized group does not enhance both the ionic conductivity and mechanical property. **Figure 46** (a) shows the DSC thermal gram of ionized graft polyrotaxane based SPE. A relatively large binary peak can be observed from 30°C to 60°C which is probably a combination of the crystallization of PEG and PCL. The ionized group may attract each other and induce the crystallization of both PEG and PCL as shown in **Figure 46** (b) and leads to the low ionic conductivity.

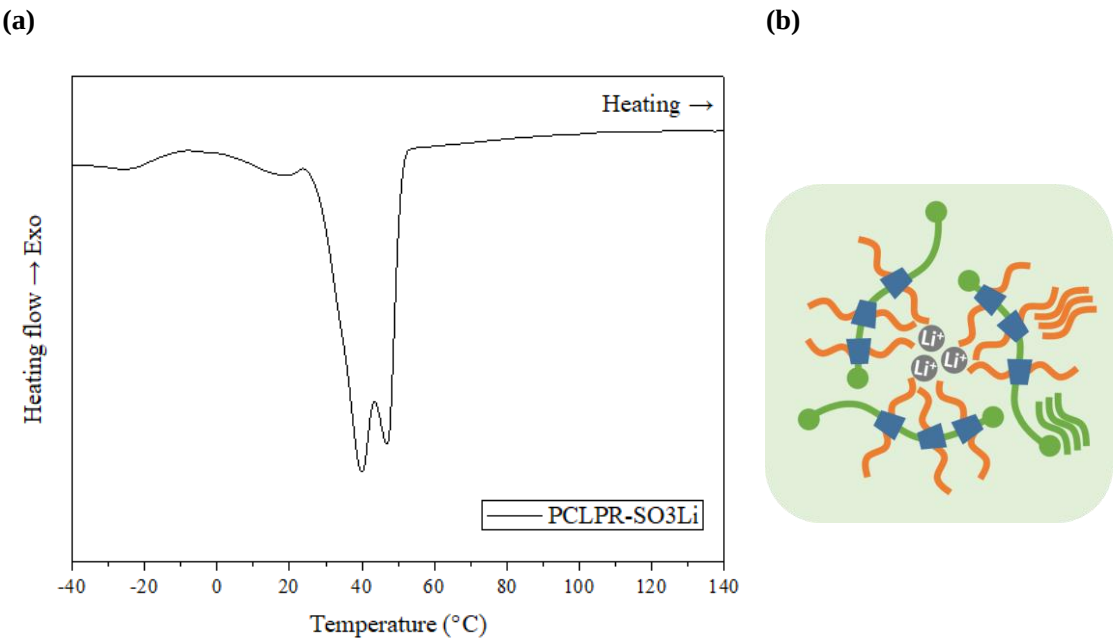

Figure 46. (a)The DSC thermalgram and (b) the proposed model of of ionized graft polyrotaxane based SPR

6.5 Summary

In this section, we have successfully synthesized the polyelectrolyte based on

polyrotaxane and “graft polyrotaxane” with LiOH and1,3-propane sultone. The synthesized ionized polyrotaxane was then used to fabricate the single ion conducting polymer electrolyte by hot pressing. However, both the ionic conductivity and the flexibility was poor due to the strong ionic crosslinking that restricts the mobility of polyrotaxane and induces the crystallization.

Chapter 7. Summary and future outlook

7.1 Summary

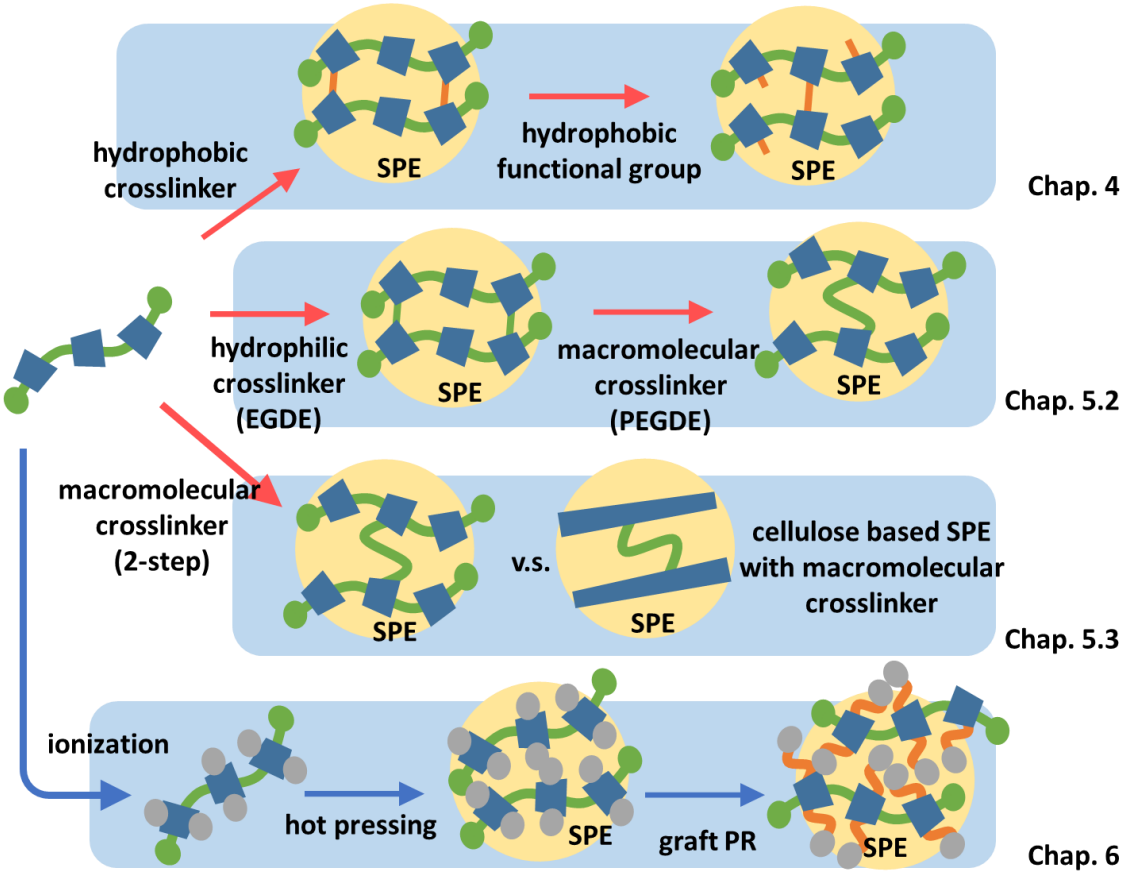

Figure 47. Summary of the research

In this research, we have prepared various polyrotaxane based SPE with different crosslinker ratio and functional groups. We found out that the low ionic conductivity of polyrotaxane based SPE was due to the hydrogen bond and the aggregation of CDs. So,

macromolecular crosslinker was applied to prevent the aggregation of CDs and hydrogen bond. The ionic conductivity of polyrotaxane based SPE was largely enhanced by using the two-step reaction to introduce more macromolecular PEG crosslinker. In the last part, the single ion conducting SPE based on polyrotaxane and graft polyrotaxane was successfully prepared but it shows low ionic conductivity. The works are summarized in Figure 47

7.2 Future Outlook

Even the prinstine polyrotaxane based SPE shows a low ionic conductivity, but we found out that the ionic conductivity can be enhanced by functionalization of the hydroxyl group on polyrotaxane or using macromolecular crosslinker. Besides the methods that we have discussed in this research, there are still some factors that affect the ionic conductivity can be studied. For example, we can modify the cover ratio of the cyclodextrins threaded on the PEG chains or we can substitute the hydroxyl groups on cyclodextrin with hydrophilic functional groups to prevent the aggregation. Moreover, we can introduce the inorganic nanoparticle to the polyrotaxane based SPE to make the nanocomposite SPE. The nanoparticle that shows large specific area[66] can not only reduce the crystallization of PEG[67] but also enhance the compatibility with the electrodes and the dissociability of the lithium salts. A recent report of our group has demonstrated that the polyrotaxane can chemically interpenetrate with the nanoparticle to form a strong and flexible nanocomposite[68]. The enhancement in chain mobility compared with conventional nanocomposite SPE can also be expected with the unique chemical structure and mobile crosslink of slide-ring nanocomposite as shown in **Figure 48** and makes it a potential material in the fabrication of SPE.

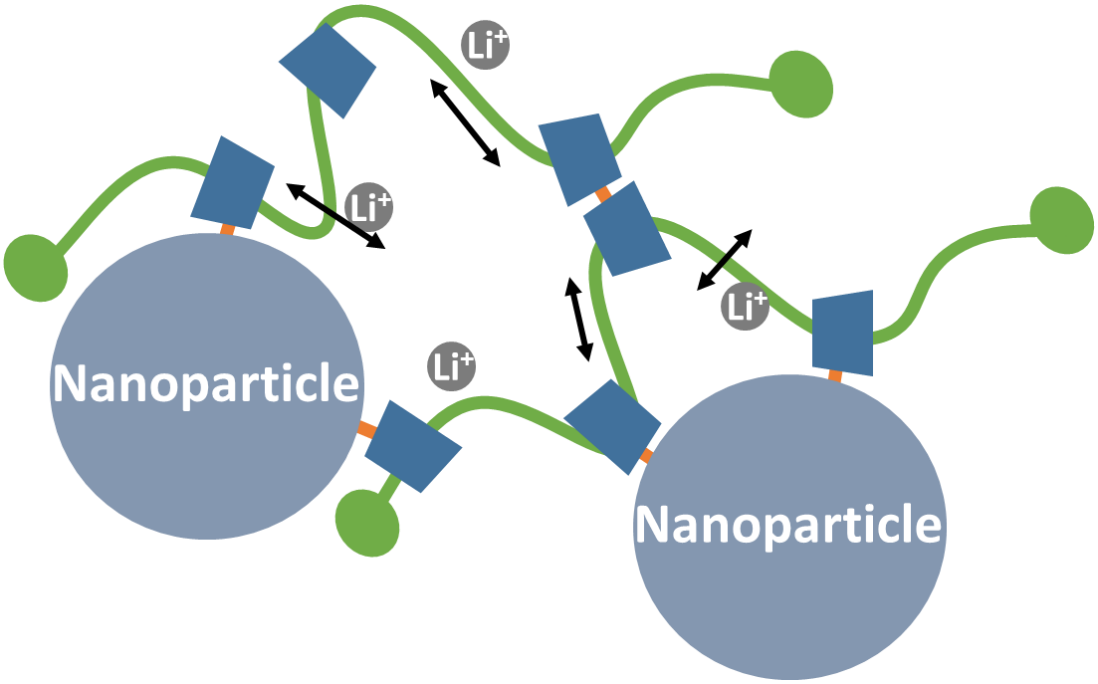

Figure 48. The nanocomposite SPE based on polyrotaxane

And we are also looking forward to the fabrication of lithium ion battery with the polyrotaxane based SPE we prepared in this research. With the fabrication of lithium battery, the transference number of lithium ion and the cycle life of battery can be studied.

References

[1] IEA, Global EV Outlook 2016 Electric Vehicles Initiative, 2016.

[2] M.A. Kiani, M.F. Mousavi, M.S. Rahmanifar, Synthesis of nano- and micro-particles of LiMn2O4: Electrochemical investigation and assessment as a cathode in li battery, Int. J. Electrochem. Sci. 6 (2011) 2581–2595. doi:10.1039/c1ee01598b.

[3] B. Scrosati, Power sources for portable electronics and hybrid cars: Lithium batteries and fuel cells, Chem. Rec. 5 (2005) 286–297. doi:10.1002/tcr.20054.

[4] D.T. Hallinan, N.P. Balsara, Polymer Electrolytes, Annu. Rev. Mater. Res. 43 (2013) 503–525. doi:10.1146/annurev-matsci-071312-121705.

[5] J.M. Tarascon, J.M. Tarascon, M. Armand, M. Armand, Issues and challenges facing rechargeable lithium batteries, Nature. 414 (2001) 359–367. doi:10.1038/35104644.

[6] D.E. Fenton, J.M. Parker, P.V. Wright, Complexes of alkali metal ions with poly(ethylene oxide), Polymer (Guildf). 14 (1973) 589.

[7] P.G. Bruce, Polymer Electrolytes, J. Chem. Soc. Faraday Trans. 89 (1993) 3187. doi:10.1039/ft9938903187.

[8] R. Khurana, J.L. Schaefer, L.A. Archer, G.W. Coates, Suppression of lithium dendrite growth using cross-linked polyethylene/poly(ethylene oxide) electrolytes: A new approach for practical lithium-metal polymer batteries, J. Am. Chem. Soc. 136 (2014) 7395–7402.

[9] Y. Liu, S. Gorgutsa, C. Santato, M. Skorobogatiy, Flexible, Solid Electrolyte-Based Lithium Battery Composed of LiFePO4 Cathode and Li4Ti5O12 Anode for Applications in Smart Textiles, J. Electrochem. Soc. 159 (2012) A349. doi:10.1149/2.020204jes.

[10] Q. Li, J. Chen, L. Fan, X. Kong, Y. Lu, Progress in Electrolytes for Rechargeable Li-based Batteries and beyond, Green Energy Environ. 1 (2016) 1–25. doi:10.1016/j.gee.2016.04.006.

[11] F. Croce, G.B. Appetecchi, L. Persi, B. Scrosati, Nanocomposite polymer electrolytes for lithium batteries, Nature. 394 (1998) 456–458. doi:10.1038/28818.

[12] P. Painter, M. Coleman, Essentials of polymer science and engineering, 2008.

[13] H. Lee, M. Yanilmaz, O. Toprakci, K. Fu, X. Zhang, A review of recent developments in membrane separators for rechargeable lithium-ion batteries, Energy Environ. Sci. 7 (2014) 3857–3886. doi:10.1039/C4EE01432D.

[14] S.S. Zhang, A review on the separators of liquid electrolyte Li-ion batteries, J. Power Sources. 164 (2007) 351–364. doi:10.1016/j.jpowsour.2006.10.065.

[15] L. Long, S. Wang, M. Xiao, Y. Meng, Polymer electrolytes for lithium polymer batteries, J. Mater. Chem. A. 4 (2016) 10038–10069. doi:10.1039/C6TA02621D.

[16] M. Armand, F. Endres, D.R. MacFarlane, H. Ohno, B. Scrosati, Ionic-liquid materials for the electrochemical challenges of the future, Nat. Mater. 8 (2009) 621–629. doi:10.1038/nmat2448.

[17] K. White, Samsung Recall Support Note7 Investigation, Expon. Press Conf. (2017) 1–9.

[18] Z. Xue, D. He, X. Xie, Poly(ethylene oxide)-based electrolytes for lithium-ion batteries, J. Mater. Chem. A. 3 (2015) 19218–19253. doi:10.1039/C5TA03471J.

[19] F. Croce, B. Scrosati, Nanocomposite lithium ion conducting membranes., Ann. N. Y. Acad. Sci. 984 (2003) 194–207. doi:10.1111/j.1749-6632.2003.tb06000.x.

[20] K. Murata, S. Izuchi, Y. Yoshihisa, An overview of the research and development of solid polymer electrolyte batteries, Electrochim. Acta. 45 (2000) 1501–1508. doi:10.1016/S0013-4686(99)00365-5.

[21] K. Cosaert, E. Eeckhout, E. Goethals, F. Du Prez, P. Guégan, H. Cheradame, Poly(ethylene oxide) containing segmented networks as precursors for ion-conducting solid-state materials, Polym. Int. 51 (2002) 1231–1237. doi:10.1002/pi.896.

[22] M. Ravi, S. Song, J. Wang, R. Nadimicherla, Z. Zhang, Preparation and characterization of biodegradable poly(??-caprolactone)-based gel polymer electrolyte films, Ionics (Kiel). 22 (2016) 661–670. doi:10.1007/s11581-015-1586-9.

[23] N. Jürgensen, J. Zimmermann, A.J. Morfa, G. Hernandez-Sosa, Biodegradable Polycaprolactone as Ion Solvating Polymer for Solution-Processed Light-Emitting Electrochemical Cells, Sci. Rep. 6 (2016) 36643. doi:10.1038/srep36643.

[24] J.Y. Song, Y.Y. Wang, C.C. Wan, Review of gel-type polymer electrolytes for lithium-ion batteries, J. Power Sources. 77 (1999) 183–197. doi:10.1016/S0378-

7753(98)00193-1.

[25] R. Bouchet, S. Maria, R. Meziane, Single-ion BAB triblock copolymers as highly efficient electrolytes for lithium-metal batteries, Nat. Mater. 12 (2013) 452–457. doi:10.1038/namt3602.

[26] P.R. Ashton, M. Grognuz, A.M.Z. Slawin, J. Fraser Stoddart, D.J. Williams, The template-directed synthesis of a [2]rotaxane, Tetrahedron Lett. 32 (1991) 6235–6238. doi:10.1016/0040-4039(91)80797-A.

[27] O. Ramström, Scientific Background on the Nobel Prize in Chemistry 2011. The Discovery of Quasicrystals, R. Swedish Acad. Sci. 50005 (2016) 1–14.

[28] C.O. Dietrich-Buchecker, J.P. Sauvage, J.M. Kern, Templated synthesis of interlocked macrocyclic ligands: the catenands, J. Am. Chem. Soc. 106 (1984) 3043–3045. doi:10.1021/ja00322a055.

[29] A. Harada, J. Li, M. Kamachi, Preparation and Characterization of a Polyrotaxane Consisting of Monodisperse Poly(ethylene glycol) and .alpha.-Cyclodextrins, J. Am. Chem. Soc. 116 (1994) 3192–3196. doi:10.1021/ja00087a004.

[30] N. Yui, T. Ooya, Design of polyrotaxanes as supramolecular conjugates for cells and tissues., J. Artif. Organs. 7 (2004) 62–8. doi:10.1007/s10047-004-0253-0.

[31] J.J. Li, F. Zhao, J. Li, Polyrotaxanes for applications in life science and biotechnology, Appl. Microbiol. Biotechnol. 90 (2011) 427–443. doi:10.1007/s00253-010-3037-x.

[32] Y. Okumura, K. Ito, The polyrotaxane gel: A topological gel by figure-of-eight cross-links, Adv. Mater. 13 (2001) 485–487.

[33] K. Ito, K. Kato, K. Mayumi, Polyrotaxane and Slide-ring Materials, 2015. doi:10.1039/9781782622284.

[34] L. Nissan Motor Co., Scratch-Resistance Scratch-Resistant Clear Coat Preserves a Beautiful Finish, Nissan Licens. Bussiness, Http//www.nissan-global.com/EN/LICENSE/PDF/technology01.pdf. (n.d.) 5622. http://www.nissan-global.com/EN/LICENSE/PDF/technology01.pdf.

[35] M. Nakahata, S. Mori, Y. Takashima, H. Yamaguchi, A. Harada, Self-Healing Materials Formed by Cross-Linked Polyrotaxanes with Reversible Bonds, Chem. 1 (2016) 766–775. doi:10.1016/j.chempr.2016.09.013.

[36] W. Wang, D. Zhao, J. Yang, T. Nishi, K. Ito, X. Zhao, L. Zhang, Novel Slide-

Ring Material/Natural Rubber Composites with High Damping Property, Sci. Rep. 6 (2016) 22810. doi:10.1038/srep22810.

[37] T. Murakami, B.V.K.J. Schmidt, H.R. Brown, C.J. Hawker, One-pot “click” fabrication of slide-ring gels, Macromolecules. 48 (2015) 7774–7781. doi:10.1021/acs.macromol.5b01713.

[38] S. Tsuchitani, T. Sunahara, H. Miki, Dielectric elastomer actuators using Slide-Ring Material ® with increased permittivity, Smart Mater. Struct. 24 (2015) 65030. doi:10.1088/0964-1726/24/6/065030.

[39] J. Son, Y. Kang, J. Won, Poly(vinyl alcohol)-based polymer electrolyte membranes containing polyrotaxane, J. Memb. Sci. 281 (2006) 345–350. doi:10.1016/j.memsci.2006.04.001.

[40] N. Sugihara, Y. Tominaga, T. Shimomura, K. Ito, Ionic conductivity and mechanical properties of slide-ring gel swollen with electrolyte solution including lithium ions, Electrochim. Acta. 169 (2015) 433–439. doi:10.1016/j.electacta.2015.04.106.

[41] N. Sugihara, K. Nishimura, H. Nishino, S. Kanehashi, K. Mayumi, Y. Tominaga, T. Shimomura, K. Ito, Ion-Conductive and Elastic Slide-Ring Gel Li Electrolytes Swollen with Ionic Liquid, Electrochim. Acta. 229 (2017) 166–172. doi:10.1016/j.electacta.2017.01.118.

[42] T. Moriyasu, T. Sakamoto, N. Sugihara, Y. Sasa, Y. Ota, T. Shimomura, Y. Sakai, K. Ito, Ionic conduction of slide-ring gel swollen with ionic liquids, Polymer (Guildf). 54 (2013) 1490–1496. doi:10.1016/j.polymer.2013.01.022.

[43] K.L. Liu, H.C. Lee, B.Y. Wang, S.J. Lue, C.Y. Lu, L.D. Tsai, J. Fang, C.Y. Chao, Sulfonated poly(styrene-block-(ethylene-ran-butylene)-block-styrene (SSEBS)-zirconium phosphate (ZrP) composite membranes for direct methanol fuel cells, J. Memb. Sci. 495 (2015) 110–120.

[44] E. Barsoukov, J.R. Macdonald, Impedance Spectroscopy Theory, Experiment, and Applications, 2005. http://books.google.com/books?hl=en&lr=&id=StDjdRnT72AC&oi=fnd&pg=PR9&dq=Supersymmetry:+Theory,+Experiment,+and+Cosmology&ots=VfJ4xl4eAq&sig=sh9EfE3rqkdk6iEl0Jxpbqt9oFg.

[45] H.J. Woo, S.R. Majid, A.K. Arof, Effect of ethylene carbonate on proton conducting polymer electrolyte based on poly(??-caprolactone) (PCL), Solid State Ionics. 252 (2013) 102–108. doi:10.1016/j.ssi.2013.07.005.

[46] J. Jalili, V. Tricoli, Proton Conductance at Elevated Temperature: Formulation and Investigation of Poly(4-Styrenesulfonic Acid)/4-Aminobenzylamine/Phosphoric Acid Membranes, Front. Energy Res. 2 (2014) 1–5. doi:10.3389/fenrg.2014.00028.

[47] T.J. Singh, S. V. Bhat, Morphology and conductivity studies of a new solid polymer electrolyte: (PEG)xLiClO4, Bull. Mater. Sci. 26 (2003) 707–714. doi:10.1007/BF02706768.

[48] K. Kato, T. Mizusawa, H. Yokoyama, K. Ito, Polyrotaxane Glass: Peculiar Mechanics Attributable to the Isolated Dynamics of Different Components, J. Phys. Chem. Lett. 6 (2015) 4043–4048. doi:10.1021/acs.jpclett.5b01782.

[49] K. Kato, T. Mizusawa, H. Yokoyama, K. Ito, Effect of Topological Constraint and Confined Motions on the Viscoelasticity of Polyrotaxane Glass with Different Interactions between Rings, J. Phys. Chem. C. 121 (2017) 1861–1869. doi:10.1021/acs.jpcc.6b11362.

[50] J. Van Heumen, W. Wieczorek, M. Siekierski, J.R. Stevens, Conductivity and Morphological Studies of TPU-N&CF3S03 Polymeric Electrolytes, (1995) 15142–15152.

[51] Z. Osman, M.I. Mohd Ghazali, L. Othman, K.B. Md Isa, AC ionic conductivity and DC polarization method of lithium ion transport in PMMA–LiBF4 gel polymer electrolytes, Results Phys. 2 (2012) 1–4. doi:10.1016/j.rinp.2011.12.001.

[52] S.H. Chung, K. Such, W. Wieczorek, J.R. Stevens, An analysis of ionic conductivity in polymer electrolytes, J. Polym. Sci. Part B Polym. Phys. 32 (1994) 2733–2741. doi:10.1002/polb.1994.090321619.

[53] N. Binesh, S. V Bhat, VTF to Arrhenius Crossover in Temperature Dependence of Conductivity in (PEG)xNH4ClO4 Polymer Electrolyte, J. Polym. Sci. Part B Polym. Phys. 36 (1998) 1201–1209. doi:10.1002/(sici)1099-0488(199805)36:7<1201::aid-polb9>3.0.co;2-w.

[54] W. Wieczorek, A. Zalewska, D. Raducha, Z. Florjańczyk, J.R. Stevens, A. Ferry, P. Jacobsson, Polyether, Poly(*N* , *N* -dimethylacrylamide), and $LiClO_4$ Composite Polymeric Electrolytes, Macromolecules. 29 (1996) 143–155. doi:10.1021/ma950672n.

[55] J.K. Maranas, Polyelectrolytes for batteries: Current state of understanding, in: ACS Symp. Ser., 2012: pp. 1–17.

[56] Y. Shinohara, K. Kayashima, Y. Okumura, C. Zhao, Small-Angle X-ray Scattering Study of the Pulley Effect of Slide-Ring.pdf, Macromolecules. 39 (2006) 7386–7391.

[57] O.E. Geiculescu, B.B. Hallac, R. V. Rajagopal, S.E. Creager, D.D. Desmarteau, O. Borodin, G.D. Smith, The effect of low-molecular-weight poly(ethylene glycol) (PEG) plasticizers on the transport properties of lithium fluorosulfonimide ionic melt electrolytes, J. Phys. Chem. B. 118 (2014) 5135–5143. doi:10.1021/jp500826c.

[58] N. Katsuyama, K. Shimizu, S. Sato, J. Araki, A. Teramoto, K. Abe, K. Ito, Preparation of Polyrotaxane Fibers. Part II: Tensile Properties of Polyrotaxane Fibers Treated with Two Cross-linking Reagents, Text. Res. J. 80 (2010) 1131–1137. doi:10.1177/0040517509352522.

[59] A. Xie, M. Zhang, S.-I. Inoue, Influence of Diisocyanate on Polyurethane Elastomers Which Crosslinked by beta-Cyclodextrin, Open J. Org. Polym. Mater. 6 (2016) 99–111. doi:10.4236/ojopm.2016.63010.

[60] A. Asghar, Y. Abdul Samad, B. Singh Lalia, R. Hashaikeh, PEG based quasi-solid polymer electrolyte: Mechanically supported by networked cellulose, J. Memb. Sci. 421–422 (2012) 85–90. doi:10.1016/j.memsci.2012.06.037.

[61] L. Jabbour, R. Bongiovanni, D. Chaussy, C. Gerbaldi, D. Beneventi, Cellulose-based Li-ion batteries: A review, Cellulose. 20 (2013) 1523–1545. doi:10.1007/s10570-013-9973-8.

[62] Y.A. Samad, A. Asghar, B.S. Lalia, R. Hashaikeh, Networked cellulose entrapped and reinforced PEO-based solid polymer electrolyte for moderate temperature applications, J. Appl. Polym. Sci. 129 (2013) 2998–3006. doi:10.1002/app.39033.

[63] K. Gong, H. Wang, X. Ren, Y. Wang, J. Chen, β-Cyclodextrin-butane sulfonic acid: an efficient and reusable catalyst for the multicomponent synthesis of 1-amidoalkyl-2-naphthols under solvent-free conditions, Green Chem. 17 (2015) 3141–3147. doi:10.1039/C5GC00384A.

[64] K. Minato, K. Mayumi, R. Maeda, K. Kato, H. Yokoyama, K. Ito, Mechanical properties of supramolecular elastomers prepared from polymer-grafted polyrotaxane, Polymer (Guildf). (2017) 1–6. doi:10.1016/j.polymer.2017.02.090.

[65] B.C. Ng, H.Y. Wong, K.W. Chew, Z. Osman, Development and Characterization of Poly-ε-Caprolactone- Based Polymer Electrolyte for Lithium Rechargeable

Battery, Polymer (Guildf). 6 (2011) 4355–4364.

[66] B. Kumar, L.G. Scanlon, Polymer-ceramic composite electrolytes: conductivity and thermal history effects, Solid State Ionics. 124 (1999) 239–254. doi:10.1016/S0167-2738(99)00148-4.

[67] B. Kumar, S.J. Rodrigues, L.G. Scanlon, Ionic Conductivity of Polymer-Ceramic Composites, J. Electrochem. Soc. 148 (2001) A1191. doi:10.1149/1.1403729.

[68] L. Jiang, K. Kato, K. Mayumi, H. Yokoyama, K. Ito, One-Pot Synthesis and Characterization of Polyrotaxane–Silica Hybrid Aerogel, ACS Macro Lett. 6 (2017) 281–286. doi:10.1021/acsmacrolett.7b00014.